Spring 1989

Design of a gear driven anti-twister mechanism for a seal-less blood processor

Ajit Nachiket Dastane
New Jersey Institute of Technology

DESIGN OF A GEAR DRIVEN ANTI-TWISTER MECHANISM FOR A SEAL-LESS BLOOD PROCESSOR

by
Ajit Nachiket Dastane

A Thesis
submitted to the Faculty of the Graduate Division of the
New Jersey Institute of Technology
in partial fulfillment of the requirements for the degree of
Master of Science in Mechanical Engineering
1989

APPROVAL SHEET

Title of Thesis: Design of a Gear Driven Anti-Twister Mechanism for a Seal-Less Blood Processor

Name of Candidate: Ajit Nachiket Dastane
Master of Science in Mechanical Engineering
1989

Thesis and Abstract Approved:

Dr.Sam Sofer, Professor, and Sponsored Chair in Biotechnology — Date

Dr.Harry Herman, Professor Asst. Chairman, Mechanical Engineering Department — Date

Signatures of other members of the thesis committee.

Dr.Raj S. Sodhi, Associate Professor, Mechanical Engineering Department — Date

VITA

Name: Ajit Nachiket Dastane

Degree and Date to be Conferred: MSME, 1989.

Secondary Education: Sir Purshurambhau College, Pune, Maharashtra, India.

Collegiate Institutions attended	Dates	Degree	Date of Degree
New Jersey Institute of Technology, Newark, NJ.	Sept 1986 to May 1989	M.S.	May 1989
M.S. University, Baroda, India.	Sept 1980 to Dec 1985.	B.E.	April 1986

Major: Mechanical Engineering

ABSTRACT

Title of the Thesis: Design of a Gear Driven Anti-Twister Mechanism for a Seal-Less Blood Processor.

Ajit N.Dastane, Master of Science in Mechanical Engineering, 1989

Thesis directed by: Dr. Sam S. Sofer, Professor, and Sponsored Chair in Biotechnology

This thesis presents the design of a gear driven anti-twister mechanism for a blood cell separator. The anti-twister mechanism allows for continuous feed and discharge lines that are rigidly attached to the rotating centrifuge head, thus eliminating the need of rotating seals. It is anticipated that the device using a gear driven anti-twister mechanism will have smoother power transmission and closer rpm tolerances.

In addition, a procedure for the dynamic analysis of the existing device, which uses a belt-driven anti-twister mechanism, is developed. The experimental values obtained

from the device are compared with the theoretical values obtained by analytical methods. This comparison demonstrates that the procedure employed can be used in prognosis of natural frequencies for devices with similar configuration. Such a dynamic analysis is important to ensure that the separator designed will not have any natural frequencies near to the operating frequencies.

ACKNOWLEDGEMENT

I wish to express sincere gratitude to Professor Sam Sofer for his guidance and moral support throughout the research. Without his advise and encouragement this work would never be possible.

I would like to express special gratitude to Professor Harry Herman. I am thankful to him for helping me to become an engineer that I so desired.

Special thanks are also due to Dr. Raj Sodhi for serving as my committee member.

The support of Emilia Rus, Tim Roche, Dinesh Sachdeva, and other colleagues in the lab is greatly appreciated. Special mention of Anju Nagpal is deserved for sharing my drawing work.

Last but not least, I wish to express special thanks to my parents. Their graciousness, understanding, and motivation played a major role in achieving my goal.

TABLE OF CONTENTS

LIST OF FIGURES

CHAPTER I

Introduction

In order to understand the need for continuous seal-less centrifuges for blood cell separations, we need to review the properties of blood, the role of centrifuges in certain treatments, and the particular need for continuous seal-less centrifuges in this connection.

NATURE OF BLOOD:

Blood is a complex fluid made up of living cells suspended in a continuous medium, the plasma. Three major particle types present in the blood are; red blood cells (RBC), white blood cells (WBC) and platelets. Red blood cells constitute 97% of the total cell volume of the blood. The normal volume fraction (hematocrit) of the red cells in human blood is about 42 to 45 percent. Plasma is a complex solution of organic compounds, inorganic salts, and organic macromolecules in water.

(i) Red Blood Cells

The major function of RBC, also called erythrocytes, is to transport oxygen from the lungs, via a protein called hemoglobin, to different tissues of the body. The RBC is shaped like a biconcave disc, with a mean diameter of approximately 8 microns, a thickness of 2 microns at the

thickest point, and 1 micron or less at the center (1).

Since erythrocytes lack nuclei and organelles they cannot reproduce, nor can they maintain the normal integrity of the cell wall with the deterioration of essential enzymes. Over a period of time, these cells age and die. Yet the total volume of circulating erythrocytes within the body essentially remains constant. The lost or dead RBC's are replenished by the bone marrow, which is the site of RBC production. The production of RBC by bone marrow fluctuates. In cases of severe erythrocyte destruction, the rate of erythrocyte production increases, to keep the total volume of circulating erythrocytes constant.

Erythrocytes are the densest of the three particles found in blood. RBCs settle to the bottom when blood is allowed to stand still, because they have a higher specific gravity than plasma, and they tend to aggregate to form rouleau. This settling rate is referred to as sedimentation velocity. When RBCs are affected in certain diseases the sedimentation rate changes, primarily because of the change in the physical characteristics of the sedimenting cells, or because of the formation of aggregates by clumping and stacking. These aggregates are called rouleax.

(ii) White Blood Cells:

White blood cells are also called as leukocytes. The major function of these cells is to provide an immune response for the body. White blood cells also originate in

bone marrow, but develop further in the lymph tissue and the thymus. Once fully developed, the circulatory system transports them to the places where they are used. The concentration of leukocytes in blood is approximately 7000 cells/mm^3. There are six different types of leukocytes normally found in blood. These are classified as either granular or agranular, depending on the presence or absence of granules in the cytoplasm.

Polymorphonuclear granulocytes are those which have lobulated nuclei and membrane bound granules. These are further classified as neutrophils and eosinphils. Neutrophils, as their name suggests, do not show preference to any particular identification dye. These are responsible for phagocytic activity. Eosinphils show preference to the red identification dye eosin, and are responsible for allergic reaction.

The next type of leukocytes called monocytes are larger than granulocytes. They themselves may function as phagocytes or may be transformed into macrophages, which is another type of phagocytic cell.

The last class of leukocytes are the lymphocytes. The major types of lymphocytes are B and T. Though both lymphocytes look the same when viewed under the microscope, functionally these cells are divided into two separate populations. One is responsible for the cellular immunity,

while the second population is responsible for humoral immunity. The T lymphocytes are those which migrate to and are processed in the thymus glands and are responsible for cellular immunity. The B lymphocytes are those which form antibodies and are further processed in some unknown area in the body. These are responsible for humoral immunity.

The normal percentage of different types of WBC in humans are:

a) Polymorphonuclear neutrophils	62.0%
b) Polymorphonuclear eosinphils	2.3%
c) Polymorphonuclear basophils	0.4%
d) Monocytes	5.3%
e) Lymphocytes	30.0%

(iii) Platelets:

Platelets are the smallest cellular elements consisting of numerous granules. They are colorless and approximately 250 million platelets/ml are present in blood. Their major functions are:

a) to form platelet plugs to stop hemorrhage from very small vessels, in particular capillaries, and,

b) releasing clotting factor which helps to accelerate the formation of fibrin necessary for clot formation.

Important physical properties of human blood are listed in Table 1.

BLOOD COMPONENT THERAPY:

Using the isolated cellular elements of blood for

TABLE 1 (11)

Physical Properties of Human Blood
(Normal Adult Mean Values)

Whole blood	
pH	7.35-7.40
Viscosity (37°C)	3.0 cP (at high shear rate)
Specific gravity (25/4°C)	1.056
Venous hematocrit-Male	0.47
Female	0.42
Whole blood volume	= 78 ml/kg body wt.
Plasma or Serum	
Colloid osmotic pressure	= 330 mm H_2O
pH	7.3-7.5
Viscosity (37°C)	1.2 cP
Specific gravity (24/4°C)	1.0239
Formed elements	
Erythrocytes	
pH	7.396
Specific gravity (25/4°C)	1.098
Count-Male	5.4 x 10^9 /ml whole blood
Female	4.8 x 10^9 /ml whole blood
Mean corpuscular volume	87 um^3
Diameter	8.4 um
Maximum thickness	2.4 um
Minimum thickness	1.0 um
Surface area	163 um^2
Life span	120 days
Production rate	4.5 x 10^7/ml whole blood/day
Hemoglobin concentration	0.335 g/ml erythrocyte
Leukocytes	
Count	= 7.4 x 10^6 /ml whole blood
Diameter	7-20 um
Platelets	
Count	= 2.8 x 10^8 /ml whole blood
Diameter	= 2-5 um

therapeutic treatment has become an important discipline in clinical medicine. The major area where such a treatment is used is in combating infection. Among those suffering from infections are burn patients whose skin is injured to the point that bacteria pass directly into the blood stream. Other examples of serious infections are patients afflicted with hematological malignancies like leukemia, and patients suffering from internal trauma.

Conventional methods used in treating such infections have been administering antibiotics or plasma expanders, like dextran or saline solution. But the fatality rate reported for the patients, on whom conventional methods are used, is high. This is because many of these infections have been caused by gram negative bacteria. These bacteria secrete a toxic lipopolysaccharide (LPS) from their cell walls . In traditional treatments, even if the antibiotic is successful in killing the bacteria, the LPS may still be released, causing shock and ultimately death. Moreover, members of gram negative bacterial strains have been known to develop immunity to antibiotics used to combat them (1).

Because of lack of success of the conventional methods of treatment, scientists are looking for alternative treatment procedures. One school of thought is to physically remove the toxic substance released by the bacteria, by using hemoperfusion through absorbents like charcoal or through ultrafiltration techniques. Physical removal methods have not

treatment methods. Further research is needed to refine and improve these clinical techniques.

Another line of thought involves increasing the circulating WBC count to give a "shot in the arm" to the body's defense mechanism. Experiments performed using these methods have shown increased survival times for experimental animals infected with gram negative bacteria or endotoxin. Increased WBC counts can be accomplished by either administering cortical steroids, such as methylprednisolone, or by transfusing large quantities of viable granulocytes, since their function is generally phagocytic in nature. Granulocyte-transfusion therapy has potential, provided collection procedures are improved (1).

GRANULOCYTE COLLECTING TECHNIQUES:

The major techniques currently used for granulocyte collection are continuous flow centrifugation leukapheresis (CFCL) and filtration leukapheresis (FL)(1,2). Both techniques have been successfully adopted to collect as much as one billion granulocytes over a period of 4 hours. Since the requirement of granulocytes is of the order of 10^{10} cells, the granulocyte yield must be increased. Methods to do this, via pretreatment with steroids or sedimenting agents are discussed elsewhere (2). The major problem faced by collection procedures is functional and morphological abnormalities caused to the granulocytes and platelets. These abnormalities can lead to side symptoms like chills, fever, and shortness of

breath in both donors and recipients.

In comparison to FL techniques, CFCL and IFL cause relatively few side symptoms (2). Also, granulocyte yield from these techniques is free from morphological or functional abnormalities Unfortunately centrifugation processes are less attractive due to lower yields and higher costs.

The lower yield problem in CFCL can be overcome by either operating the continuous flow centrifuge at higher centrifuge speeds, higher blood flow rate, and higher collection efficiencies or by increasing the residence time of the blood in the separation chamber(3,4).

Increased shear stress is induced by the passage of blood through rotating seals. Besides platelet damage, and other complications like frequent leakages and inter-communication between blood fractions through the rotating seals are also encountered.

One method to reduce the shear-induced damage to cellular components in continuous centrifugation procedures is to eliminate the necessity of a rotating seal(2). If this source of shear stress is eliminated then the range of operation of the device will not be restricted to the low shear-stress regimes. The expansion of operating conditions will not only allow more blood to be processed in a given time, but will enhance the potential of the device for application of the process in other areas(2,3).

Recent developments in the search for an alternative for

the rotating seal lead to the design of a centrifuge with an anti-twister mechanism. Major work on this design was carried out by Ito and Kolobow of NIH (2). An Anti-twister mechanism makes it possible to connect flexible tubes directly to the rotating centrifuge head avoiding any rotating seal. No twisting or shearing of the tubes is observed when using the anti-twister, even at very high angular velocities.

This kind of sealless centrifuge has shown a great improvement over the conventional centrifuge with rotating seals. Experiments performed using the device with an anti-twister mechanism have shown little or no platelet damage. Moreover, there was no adverse reaction to experimental animals, even after continuous operation for 24 hours at almost twice the rpm and twice the flow rate (2).

CHAPTER II

Objectives

The Blood Processing Group at the NJIT Biotechnology Laboratory is an inter-disciplinary group. It consists of engineers with electrical, chemical, mechanical, and biomedical backgrounds. The primary aim of this group is to develop a dynamic centrifugation device for high efficiency and high resolution blood processing with all associated controls. Presently, this group is involved in developing an extracorporeal detoxifier to remove diseased white cells, which has a potential application in the treatment of AIDS and Cancer. The experimental extracorporeal device is a centrifugal cell separator, which can be used to collect and separate different blood components.

Major efforts in this group involve designing and building different centrifuge heads and separation chambers for single stage, as well as multi-stage, operation of the device.

In determining the shape of the chamber, the fluid mechanics involved in blood flow and its effect on the sedimentation velocities of each cellular component of blood play an important role. Continuous efforts are also required in designing and developing separators with improved anti-twister mechanisms allowing higher centrifuge speeds. Some other mechanical problems which call for attention are,

breaking of the flexible tubing lines at the connection point to the chamber, tensile forces on the multi-lumen tubing, breaking of the fiber optics and sensor lines, and biocompatibility and sterilizability of the materials. Finally, once the device gives the desired results, the prototype will have to be rebuilt keeping mass production in mind.

The work presented here concentrates on the antitwister portion and was carried out in conjunction with Dr. Harry Herman of the Mechanical Engineering department at NJIT. In this thesis a centrifugal cell separator with gear driven anti-twister mechanism is designed. Detailed drawings of each component of the separator are presented. Static analysis is carried out to determine imbalances in the device which will affect the performance.

Finally a procedure to determine the natural frequency of such a device is developed. This procedure has been applied to the existing device and analytical results compared with the experimental results. A similar procedure can be carried out to determine the dynamic behavior of the proposed device. Specifically, the lowest natural frequencies of the device have to be found and checked against the operating frequencies to ensure that there is no resonance in the operating regime of the blood processor.

CHAPTER III

Anti-Twister Mechanism

Principle of Anti-twister Mechanism:

The anti-twister mechanism was first developed by Adams and was patented for use in supplying electrical contacts to a rotating device with continuous wires, though a similar mechanism was used by shoe lace makers in olden days. Since then researchers have successfully used the concept in continuous centrifugation processes to eliminate rotating seals.

The principle could be understood (5) by imagining a flexible tube attached at one end to a solid support. The tube is attached at the other end to a hollow shaft which in itself is mounted on some carrier. If the carrier is rotating at an angular velocity of +w, then to prevent the tube from twisting, the hollow shaft will have to rotate at a angular velocity of -w with respect to the carrier. Furthermore, if the remaining length of the tube is looped and passed through the hole at the center of the carrier and the free end of the tube is allowed to rotate independently from the carrier then the free end will have an angular velocity of +2w.

This means that, to have a continuous line from the rotating centrifuge head to the patient, the ratio of angular velocity between the head and the carrier has to be 2.

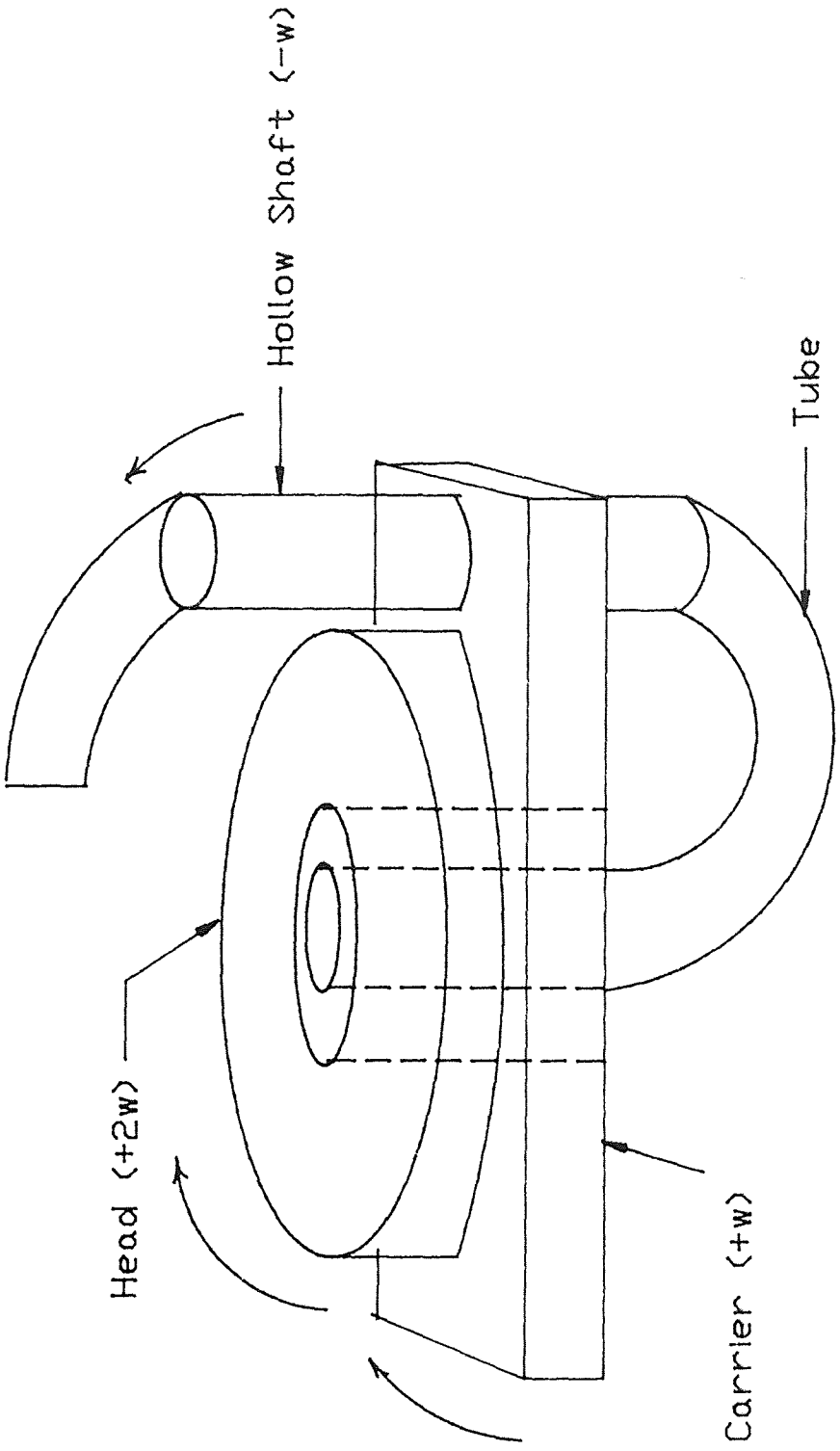

Fig. 1(a) Anti-Twister Mechanism

Gear Driven Anti-twister Mechanism:

Figure 1 represents an all gear anti-twister mechanism. The ratio of 2 between angular velocity of the centrifuge head and the carrier can be maintained provided proper selection of teeth is done for the gears. This is so because the teeth ratio of the meshing pair of gears also represents the speed ratio for that pair.

In the configuration shown, there are three principal elements: two independently rotating coaxial gears and a rotating carrier.

If carrier 'C' is fixed then the speed ratio between gear 'B' and gear 'A' can be written as,

R_{AB} = Speed of A/ Speed of B

or

R_{BA} = Speed of B/ Speed of A

The speed ratio can be easily calculated from the number of teeth on each gear. In the figure let T_A, T_B, T_E, T_F, and T_G represent the number of teeth on the respective gears, A,B,E,F and G. In terms of number of teeth, the speed ratio R_{AB} between gears A and B can be written as,

R_{AB} = product of number of teeth on followers, and
product of number of teeth on drivers

For the configuration shown in figure 1(b),

$$R_{AB} = - (T_B \times T_E) / (T_A \times T_F) \quad (i)$$

The negative sign in equation (i) is because of the idler gear G which reverses the direction of rotation of the gear A.

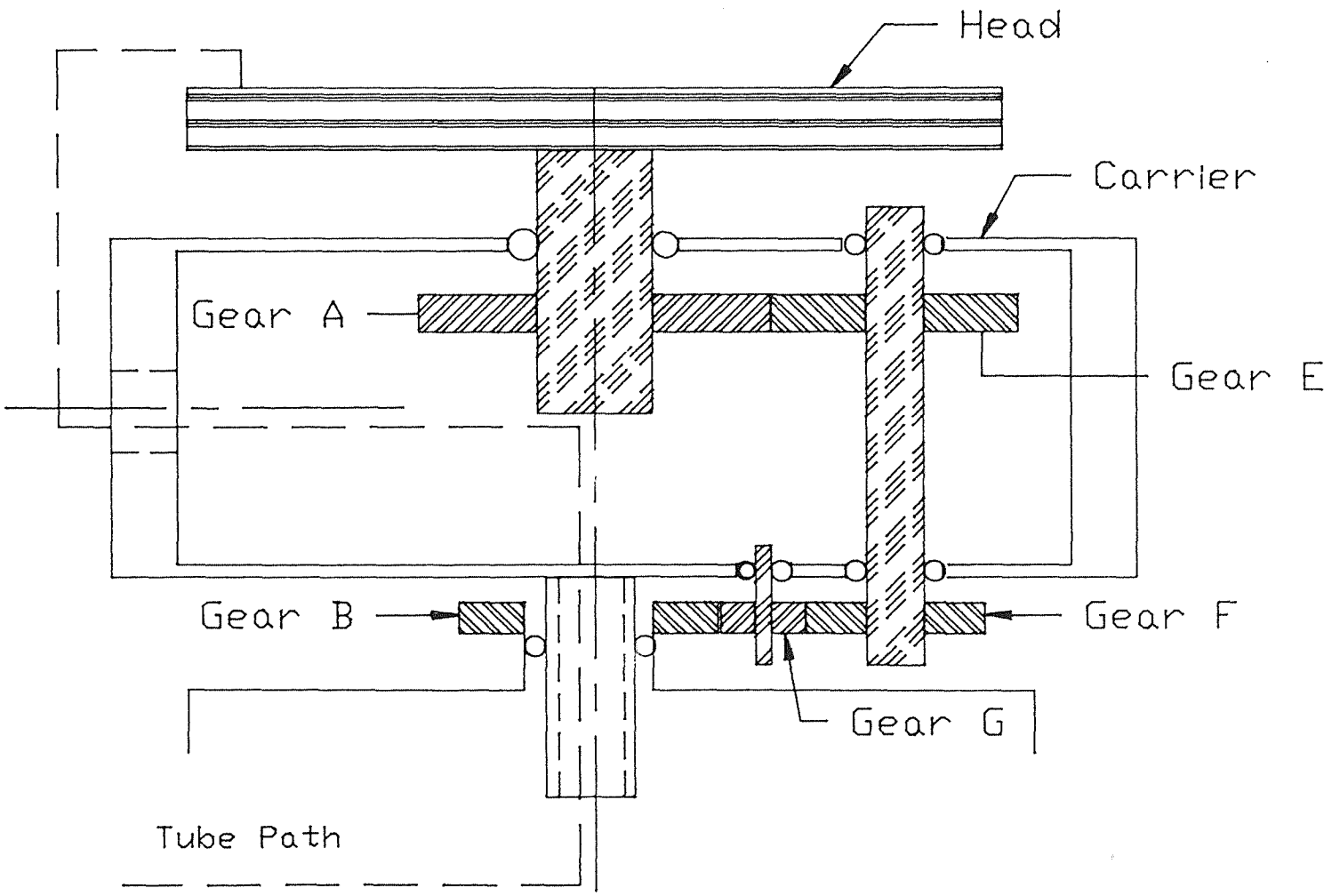

Fig. 1(b)Schematic Diagram of the Proposed Device

Configuration Analysis Steps:

To analyze the configuration, each member is rotated one revolution in the positive direction (i.e clockwise). In the second step carrier C is kept fixed and gear B is rotated one revolution in the negative direction (i.e anti-clockwise). Thus the entire configuration returns to its initial position.

These steps are tabulated below to arrive at the resultant speed of each element.

	Carrier 'C'	Gear 'B'	Gear 'A'
Step 1 :	+1	+1	+1
Step 2 :	0	-1	$-R_{AB}$
Resultant:	+1	0	$1 - R_{AB}$

Now if N_A and N_C represents the speeds of gear A and carrier C, then

$$(N_A/N_C) = 1 - R_{AB} \qquad \text{(ii)}$$

Substituting R_{AB} from (i),

$$N_A/N_C = 1 + (T_B \times T_E)/(T_A \times T_F)$$

or,

$$N_A/N_C = [(T_A \times T_F) + (T_B \times T_E)]/(T_A \times T_F) \qquad \text{(iii)}$$

For the anti-twister mechanism the ratio on the left hand side of equation (iii) has to be 2, that is to say,

$$2 = [(T_A \times T_F) + (T_B \times T_E)] / (T_A \times T_F)$$

On simplifying, the result is,

$$(T_A \times T_F) = (T_B \times T_E) \qquad \text{(iv)}$$

This indicates that the configuration shown can act as an anti-twister mechanism if the number of teeth on gears A, B, E, F satisfy equation (iv).

CHAPTER IV

Functional Analysis of the Cell Separator

Figure 2 shows the sectional elevation and the top view of the proposed device. As seen from the drawing, the device consists of the head mounted on the carrier and the gear train which is designed to give the ratio of 2 between the angular velocity of the head and the carrier. The motor drives the main shaft through the belt and pulley configuration. The main shaft is welded to the carrier, hence with the rotation of the shaft the carrier also rotates.

The carrier along with carrying the head and chamber configuration also carries the counter shaft and idler gear shaft. The counter shaft carries two gears. The top gear (i.e gear E in the figure 1(b)) meshes with the gear A on the chamber shaft, while gear F meshes with the idler gear G on the idler gear shaft. Gear G also meshes with the fixed gear B. This gear is fixed on the enclosure plate and offers the necessary reaction for the motion to occur. Further anti-friction bearings between the carrier and shafts, allow these shafts to rotate freely about their own axis. Thus these shafts while revolving about the assembly axis also rotate about their own axis.

The transmittal of the power to the head is done through the gear train in the following fashion:

If we assume that the motor drives the carrier in the

(see pocket)

clockwise direction then the idler gear G that meshes with the fixed gear B on one side, and the gear F on other side, rotates the compound gear shaft in the counterclockwise fashion. The gear E on the compound gear shaft then rotates the gear A in the clockwise fashion. The angular velocity ratio of 2 between the head and the carrier is maintained by the number of teeth on each meshing gears.

The feed and the discharge lines for the blood, that are connected to the chamber mounted on the head, first pass through the main shaft and then come out from the side of the carrier. These lines can only be connected at one point either at the top or at the bottom of the chamber. The lines will twist if these are connected in any other fashion.

Mechanical Components:

1) Carrier: The carrier is a rectangular box 10 inches long and 2.50 inches high with all sides open except top and the bottom. The detail drawing is shown in Figure 3.

As seen from the drawing, the top surface of this box has two holes, one at the center and other off-centered hole at a distance of 3 inches. Through the center hole the shaft carrying the head passes, while the off-centered hole holds the compound gear shaft.

In the bottom plate of the box there are three holes. In the center the main shaft is welded, the idler shaft is in the second hole at a center to center distance of 1.875 inches from the center hole, while the counter shaft passes through

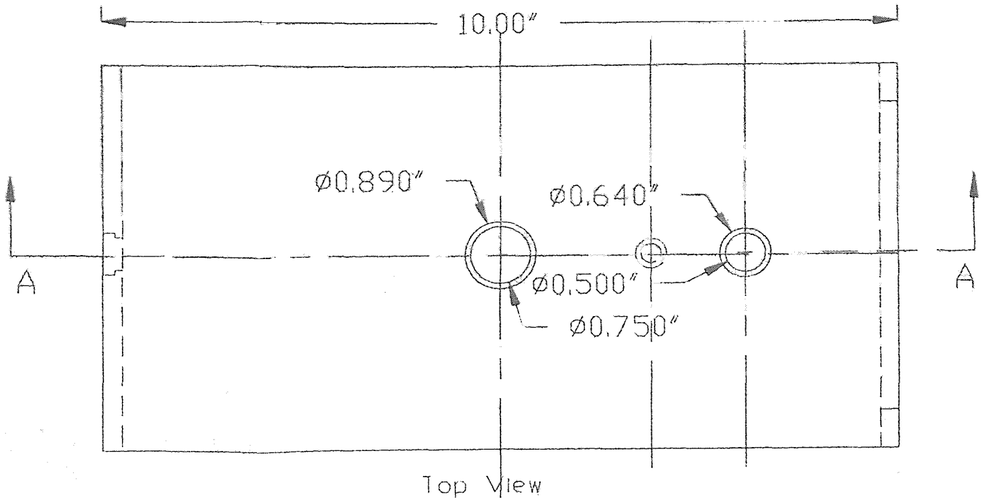

Top View

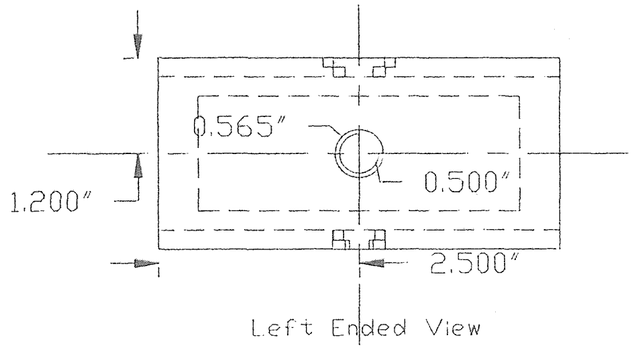

Left Ended View

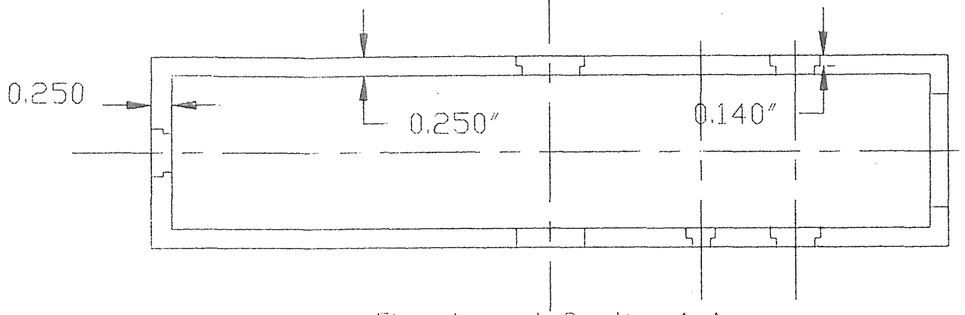

Elevation at Section A-A

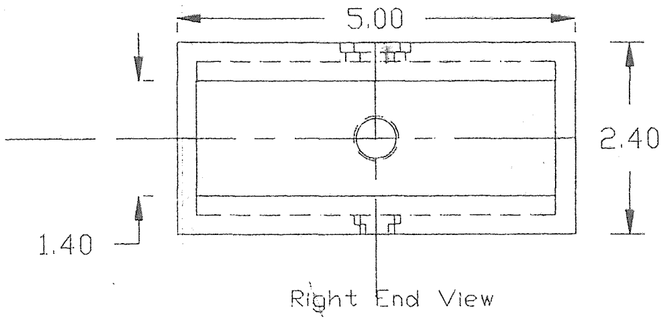

Right End View

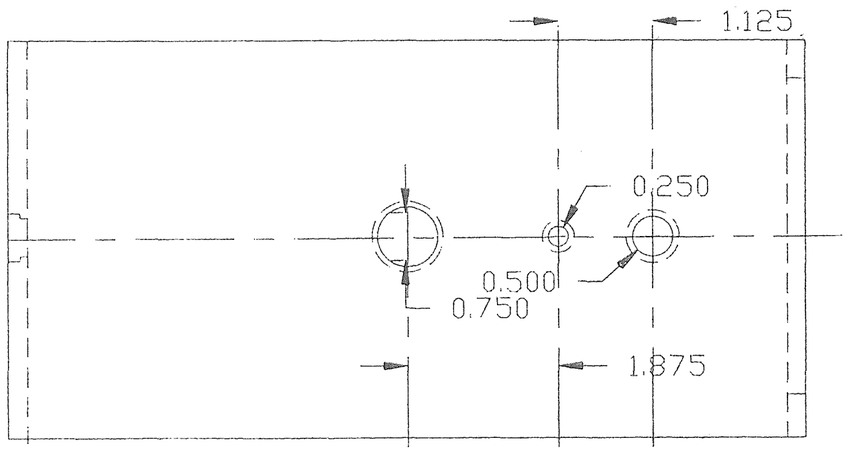

Bottom View

Material: Nylon66 impregnated with Carbon Fiber

QTY: One

Fig. 3 Details of Carrier

the third hole. The center to center distance between the center hole and the third hole is 3.00 inches. The weight of the carrier is so distributed that the imbalance about the assembly axis is minimum. This is done by increasing the thickness of one of the sides of the carrier, so that this side acts as the counter weight.

The alternative design that was thought of was the carrier with three plates viz. side, top and bottom assembled together with screws. The distances between the plates was maintained by using standoffs made up out of suitable material. But this kind of design was found to be less rigid than the proposed one, since the proposed carrier is essentially a single piece and not an assembled unit. The more rigid structure means the natural frequency of this component will be high. This in effect means, there are remote chances of the device experiencing vibrations at low rpms.

Selection of the Material: Important properties governing the selection of the material for the carrier are rigidity, weight, and cost.

One of the materials which fits this bill is carbon impregnated fibers in plastics like rayon, acrylic or polyacrylonitrile (PAN). These composites have modulli of elasticity ranging from 5 to 100 million psi. Some of the other useful properties which these materials possess is light weight, good corrosion resistance, excellent friction, wear and high temperature characteristics(6,7).

The cost per pound of these materials is dependent on the modulus of elasticity and the form in which the carbon fiber is supplied. For higher modulus and finer fiber the cost is high. But for this particular application the intermediate modulus varieties in the form of chopped fiber or tow containing about 12,000 to 50,000 is sufficient. These are priced in the range of $13 to $30 per pound.

Manufacturing method: The components made out of these composites can easily be injection molded. Injection molding allows relatively complex shapes to be manufactured with excellent dimensional tolerances. This process is especially suitable for high production runs, and can economically yield thousands of units per hour (8).

The weight, moment of inertia and the imbalance for this component is computed in Appendix(I). These are listed below:

Total Weight: 1.234 lbs.

Moment of Inertia: 4.895E-04 lb-inch-sec^2 (@ assembly axis)

Imbalance: - 0.437 lbs-inch (negative since anti clockwise)

2) Main Shaft: This is a hollow cylindrical shaft, made from carbon impregnated fiber. Figure 4 shows the details for this shaft. This shaft is welded at one end to the carrier while at other end it rests on the thrust bearing.

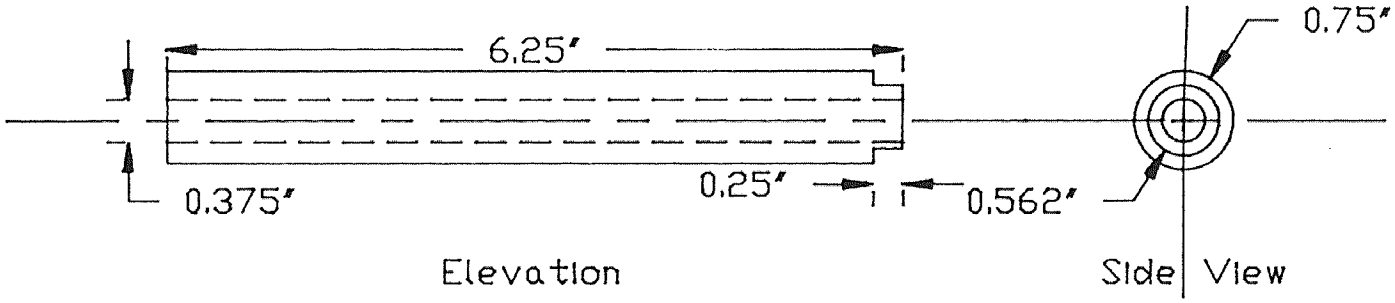

a) Main Shaft

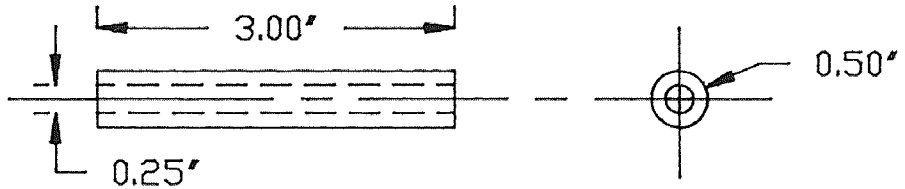

b) Compound gear shaft

Fig. 4 Details of Shafts

The mechanical properties of this shaft are listed below:

Weight: 0.093 lbs

Moment of Inertia: 2.128E-05 lb-inch-sec^2

Imbalance: 0

3) Idler gear and shaft: Idler gear selected is the standard gear available in the market with the 32 pitch and 20^0 pressure angle. Number of teeth on this gear are 24, with pitch circle diameter of 0.750". The material for the gear is Delrin.

The idler shaft is tubular in nature with wall thickness of 0.047". This shaft is similar to the compound gear shaft, except for the dimensions. The outer diameter of this shaft is 0.25 inches, inner diameter is 0.156 diameter and length is 1 inch. Material for the shaft is Teflon.

The mechanical properties of the gear and shaft assembly are listed below:

Weight: 0.0072 lbs

Moment of Inertia: 6.69E-05 lb-inch-sec^2

Imbalance: + 0.0135 lb-inches

4) Compound gears and shaft: Gears E and F form compound gears, since they are mounted on the same shaft. Both these gears are standard gears available in the market.

The Gear F has 32 pitch and 20^0 pressure angle. Number of teeth on this gear are 48 and pitch circle diameter is 1.500". Gear E has 24 pitch and 20^0 pressure angle. Number of teeth on this gear are 48 and pitch circle diameter is 2.00". Material

of both gears is Delrin.

The compound gear shaft is tubular in nature with thickness of 0.125 inches, length 3 inches and outer diameter of 0.50 inches. The material for this shaft is Teflon. Figure 4 shows the dimensional details.

The mechanical properties of the gear shaft assembly are listed below:

Weight: 0.0927 lbs

Moment of Inertia: 7.505E-05 lbs-inch-sec^2

Imbalance: + 0.2781 lb-inch.

5) Head, shaft and gear: The head is circular in shape and can be of any biocompatible translucent material like polypropylene. The chambers can be mounted on the head or can be cut in the head. For the proposed device the head is made up of 0.50"thick and 10" diameter circular plate of polypropylene. The chambers will be cut in the head. The inlet and outlet of the chamber will have small protrusions to fix the feed and discharge lines.

The shaft is a hollow cylinder with a shoulder at the bearing end. It has the thickness of 0.094" towards the thrust bearing and 0.188" towards the head end. Material for the shaft is Teflon.

Gear A is mounted rigidly on this shaft. This is a standard gear with the 24 pitch and 20^0 pressure angle. Number of teeth are 96 and pitch circle diameter is 4". Material is Delrin.

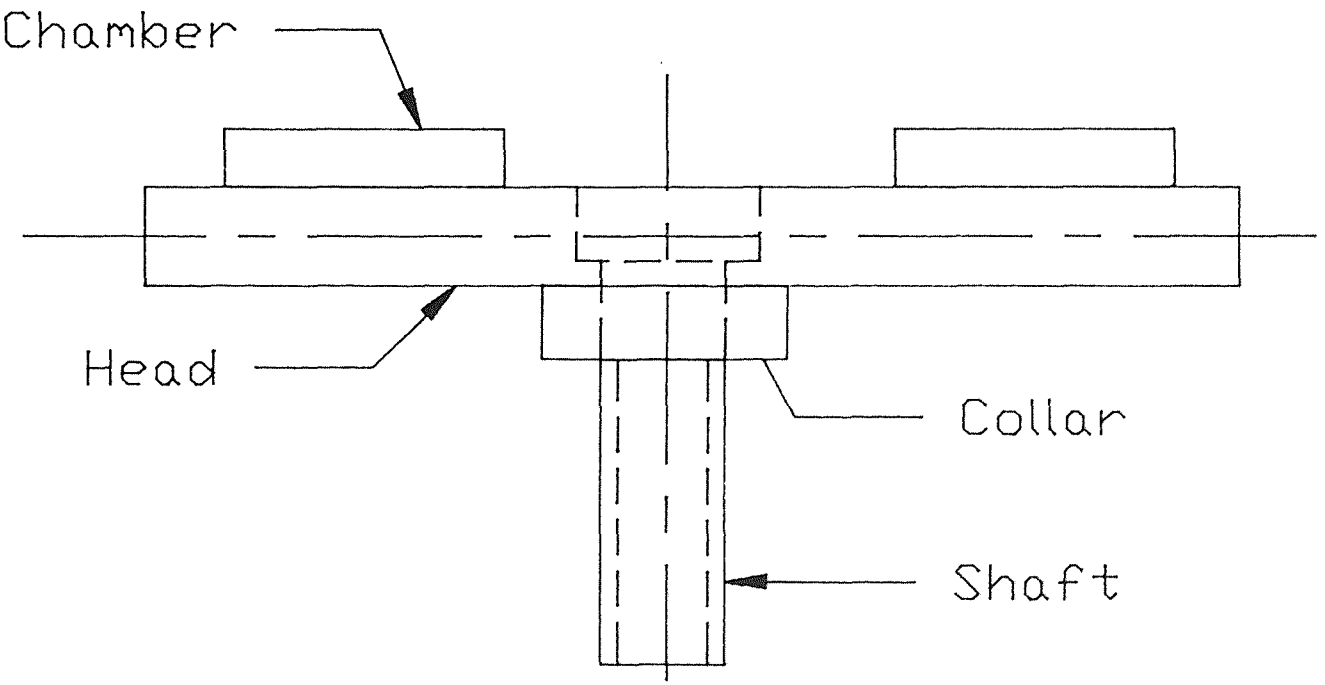

Fig. 5 Schematic of Head and Chamber assembly

Figure 5 gives the detail drawing for each of these components.

The mechanical properties of the assembly are listed below:

Weight: 1.84 lbs.

Moment of Inertia: 0.560 lbs-inch-sec^2

Imbalance: 0

6) Fixed gear: This is a nonstandard gear made from Delrin. It has 32 pitch and 20^0 pressure angle. Reason for customization of this gear is the bore in this gear has to be sufficiently large to hold the boss of the enclosure plate. The details of this gear are shown in Figure 6.

7) Retaining rings: The retaining rings are used to hold the shaft in its place. They perform the same function as that of shaft collars. Since the shaft collars are bulky we opted for retaining rings. The detail drawing of the retaining rings is shown in the Figure 7. Two retaining rings will be required; one for the idler shaft and other for the counter shaft. These retaining rings are standard and available in the market. Material for the retaining ring is carbon spring steel with oil dipped finish.

8) Anti-friction Bearings: Anti-friction bearings used are standard bearings. These are required between the carrier and the three shafts, viz, idler gear shaft, compound gear shaft and the head and chamber shaft, and the main shaft and the enclosure plate.

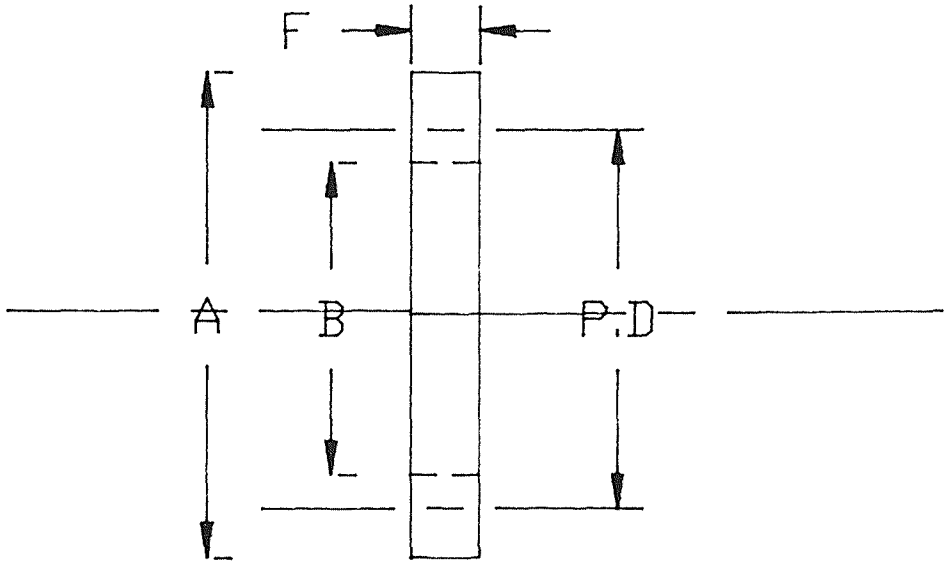

DIMENSIONAL DETAILS:

A = 4.00", B = 2.40", P.D = 3.96", F = 0.25"

No. of Teeth = 96, Pressure angle = 20, 32 pitch

Fig. 6 Fixed Gear Details

Each bearing will have rings of Delrin, cage of polyamid and balls made from ground glass. Dimensions and other details are listed in Figure 7.

a) Between the chamber shaft and the carrier: bore size 0.750 inches, outer diameter 1.62 inches, flange diameter 1.777 inches, thickness of flange 0.146 inches and height of the entire bearing will be 0.25 inches.

Same bearing will be used between the main shaft and the enclosure plate.

b) Between the counter shaft and carrier: bore size 0.25 inches, outer diameter 0.50 inches, flange diameter 0.56 inches and height of the entire bearing 0.250 inches.

c) Between the idler gear shaft and carrier: bore size 0.125 inches, outer diameter 0.25 inches, with flange 0.375 inches. Total height 0.250 inches.

9) Thrust bearing: Three thrust bearings are required; one for the head and chamber shaft, one for the main shaft and the third one for the motor shaft. These bearings will carry the thrust load. The thrust bearings used here are standard bearings available in the market and can be purchased off the shelf.

The major dimensions are, bore size 0.562 inches, outer diameter 1 inch, ball size 0.125 inches, number of balls is 6. Washer thickness is 0.062 inches and total bearing thickness is 0.249 inches. Material for retainer will be molded nylon with balls made up of ground steel (refer Fig.8).

EXTERNAL RETAINING RING DETAILS:

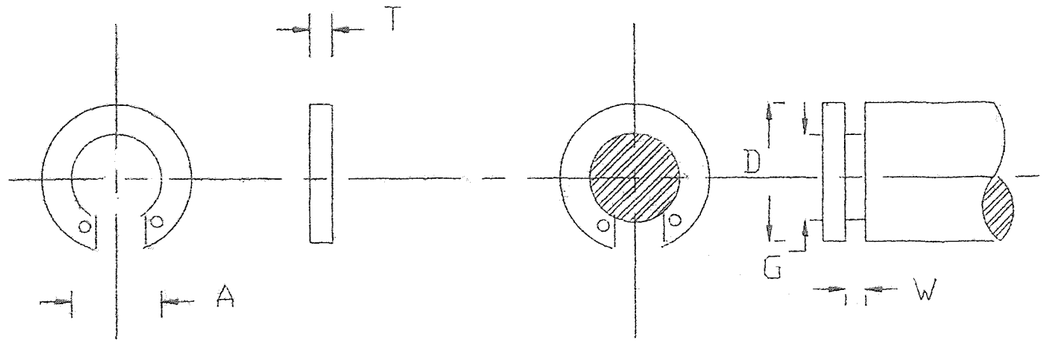

DIMENSIONAL DETAILS:

For Idler Gear Shaft: A = 0.225", T = 0.010", D = 0.250",
G = 0.23", W = 0.029"

For Counter Shaft: A = 0.461", T = 0.035", D = 0.500",
G = 0.468", W = 0.039"

MATERIAL: Carbon Spring Steel, FINISH: Oil Dipped

ANTI-FRICTION BEARING:

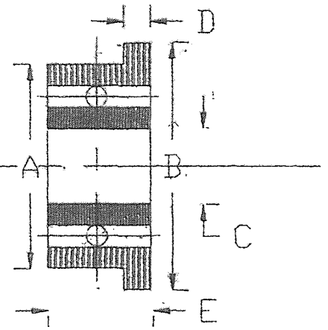

DIMENSIONAL DETAILS:

Between chamber shaft and carrier: A = 1.62", B = 1.77", C = 0.75"
D = 0.120", E = 0.250"

Between counter shaft and carrier: A = 0.50", B = 0.560", C = 0.250"
D = 0.120", E = 0.250"

Between idler gear shaft and carrier: A = 0.250", B = 0.375",
C = 0.125", D = 0.120", E = 0.250"

MATERIAL: 440C Stainless Steel

Fig. 7 Details of Anti-friction bearing and retaining ring.

THRUST BEARING:

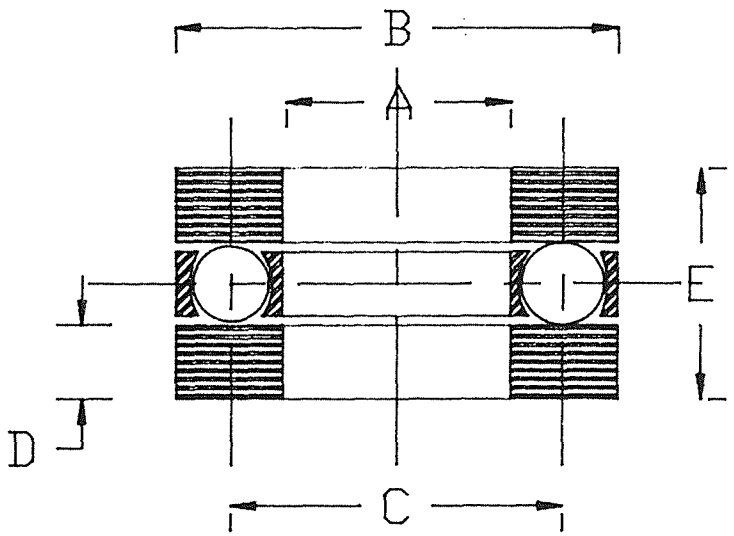

DIMENSIONAL DETAILS:

A = 0.562", B = 1.00", C = 0.781", D = 0.062", E = 0.249"

No. of Balls = 9, Ball Size = 0.125"

MATERIAL: Balls: Ground Steel, Retainer: Molded Nylon,
Washers: Hardened Steel

Fig. 8 Details of Thrust Bearing

10) Thrust Bearing Seat: These will hold the thrust bearings and will be custom made. Thrust bearing seats will be screwed to the respective supports i.e for main shaft and motor shaft and will be screwed to the enclosure, while for head shaft seat it will be screwed to the carrier.

This component will be injection molded. The dimensional details are shown in Figure 9. Material used is Nylon 66 impregnated with carbon fiber.

11) Enclosure: The enclosure for the centrifuge is a rectangular box and the dimensions for this box are 16"x16"x17". There is a plate at a distance of 9 inches from the base which divides the enclosure into two parts. The top part supports the rotating structure of the cell separator while the bottom part holds the motor and power transmitting mechanism.

The dividing plate has the bossed central hole. The main shaft of the cell separator passes through this hole and the fixed gear is attached rigidly on the periphery of the boss.

The material for the enclosure is ABS (acrylonitrile butadine styrene). ABS has good stiffness and chemical resistance, and excellent toughness. It is widely used for automotive panels and luggage and sports goods accessories because of its good appearance and moderate cost. It can be easily injection molded. Figure 10 shows the necessary details.

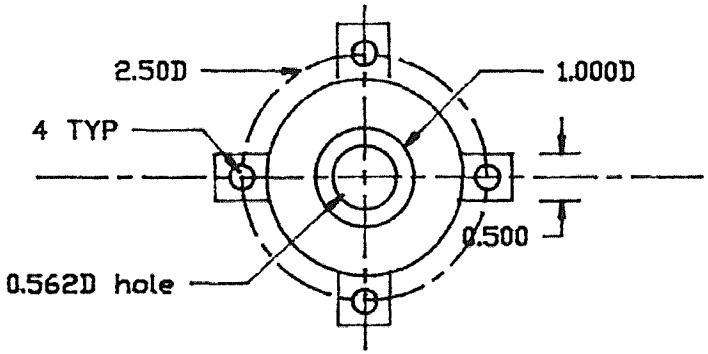

PLAN

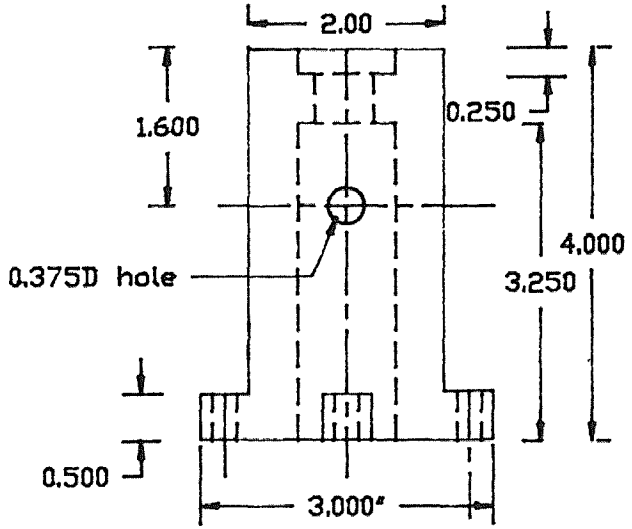

ELEVATION

COMPONENT NAME:

Thrust bearing seat

MATERIAL:

Carbon Impregnated Fiber

COMPONENT NAME:

THRUST BEARING SEAT

MATERIAL: Carbon Impregnated Fibre

ALL DIM. IN INCHES

Fig. 9 Thrust Bearing Seat for main shaft

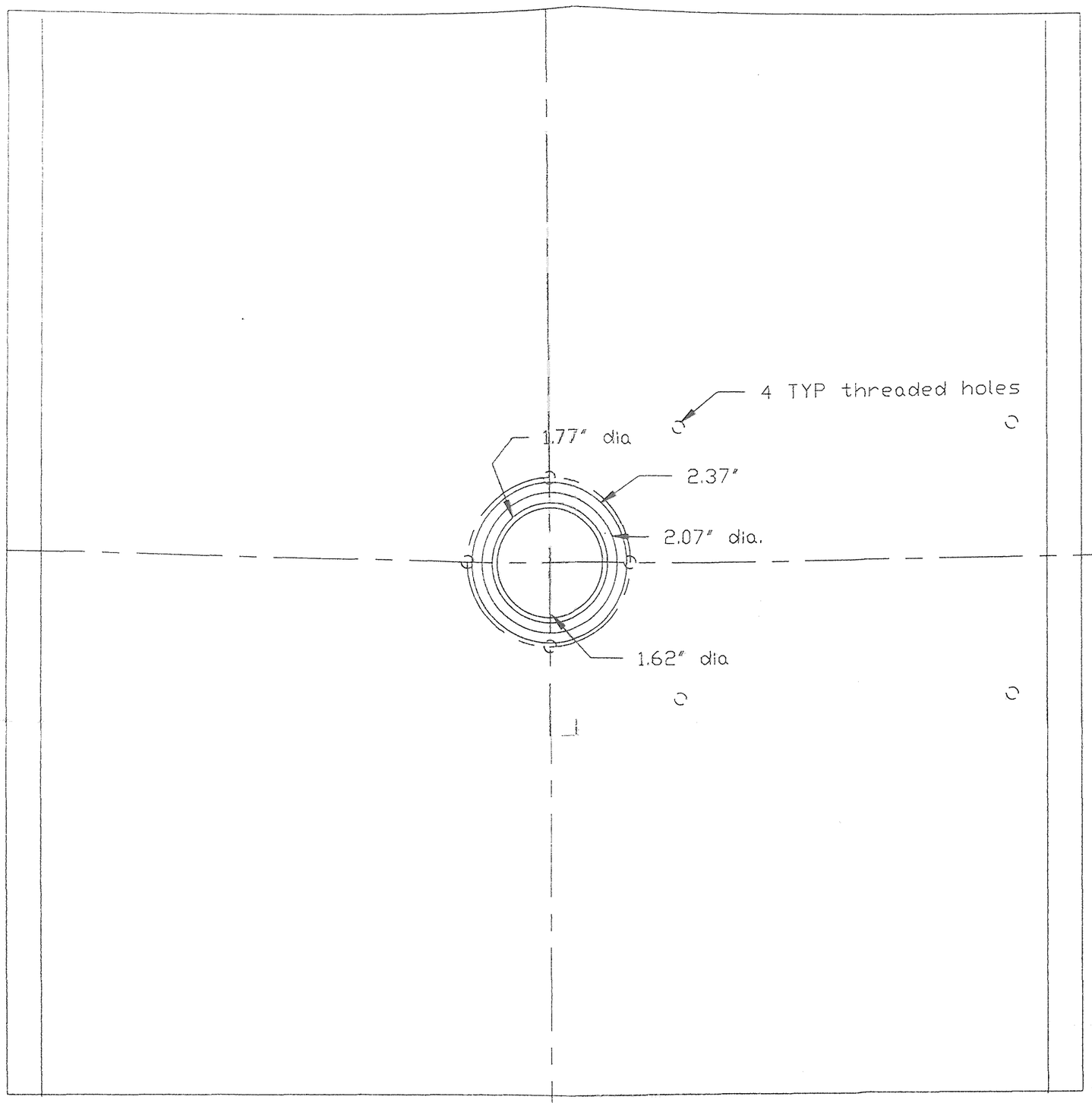

Top View

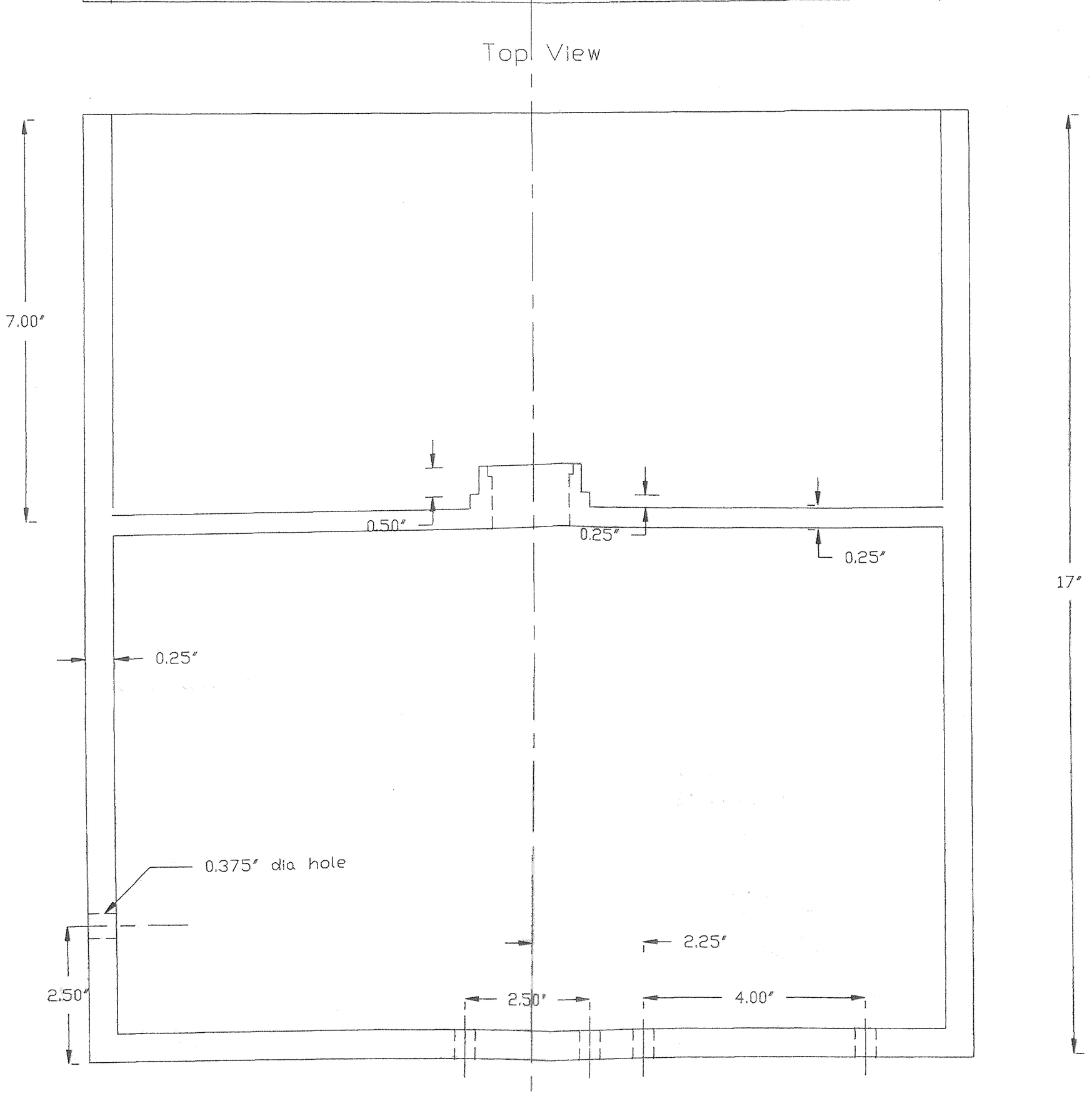

Elevation

COMPONENT NAME:

ENCLOSURE

MATERIAL: ABS

QTY: 1

FIG. 10 DETAILS OF ENCL

CHAPTER V

Dynamic Analysis of the Existing Cell Separator

The existing cell separator is a belt driven device. By this we mean that the power transmittal is achieved by timer belt and pulley arrangement. Figure 11 shows the schematic representation of the device.

As seen from the figure, the device consists of rotating head and the antitwister mechanism. The anti-twister mechanism consists of two plates, that are 12" and 6" long. The plates are stacked vertically as shown. The top plates are separated by a distance of 1/2" with 3/8" diameter aluminum spacers. The distance between the 6" long bottom plate and the lower 12" long plate is 2 inches, which is maintained by four aluminum spacers of same length and 3/8" diameter.

Power is supplied by a 1/2 HP ac motor to a 1/2" diameter stainless steel center shaft, which carries above mentioned plate configuration. Thus as shaft turns the plate structure also rotates. As the plates turn, power is transmitted to a second 1/4" solid aluminum shaft, which rotates at an angular velocity of -w, if the plates are turning at +w. The power transmittal is achieved by the timing belt and pulley arrangement.

The second shaft transmits power to the hollow center shaft that carries head and chamber, through the spur gears (3" dia, 12 pitch). This rotates head and chamber at an angular velocity of +2w.

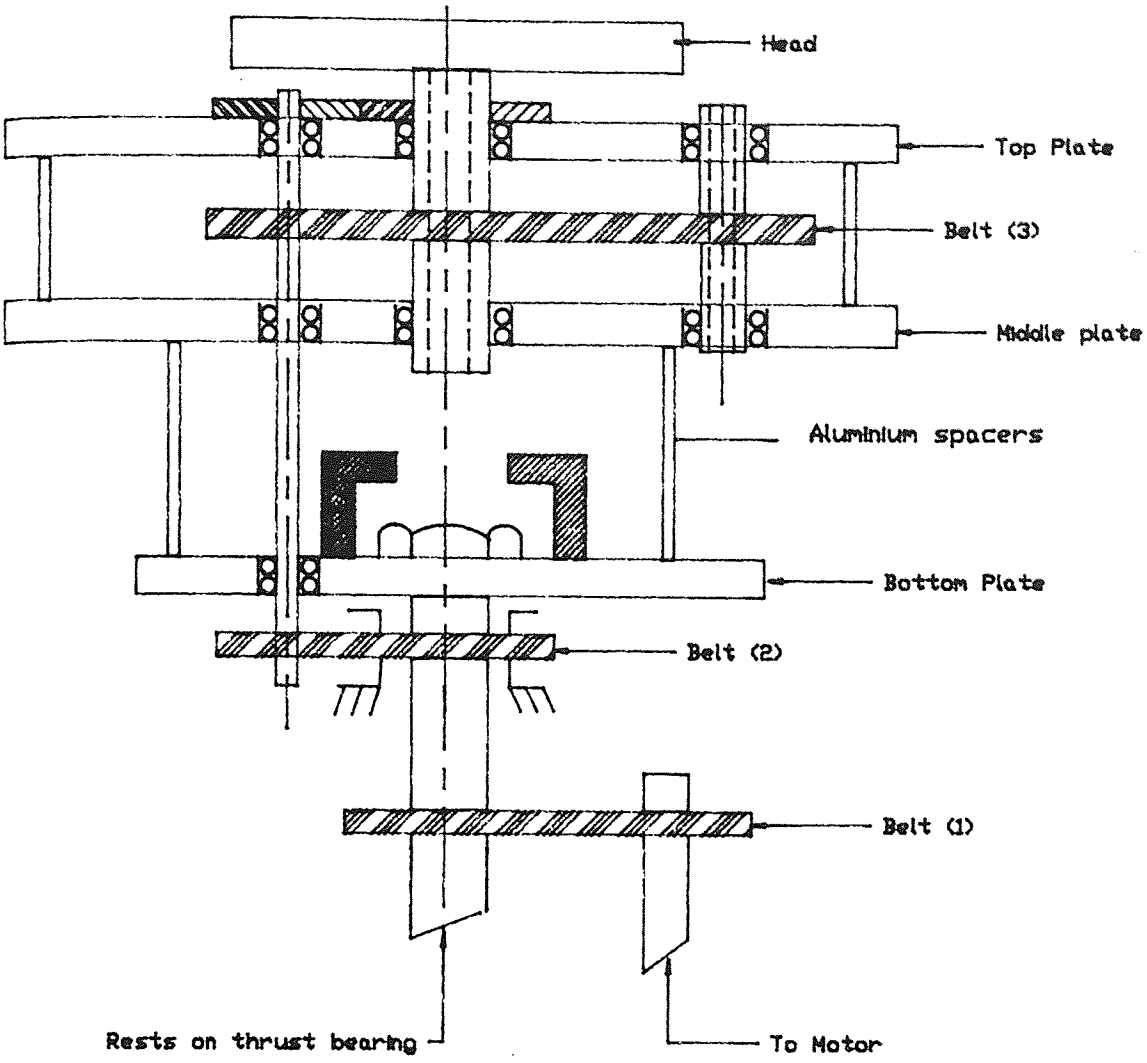

Fig. 11 Schematic of the existing cell separator

The second shaft also transmits power to the hollow fourth shaft through an open timer belt and pulley arrangement. Thus the hollow shaft rotates at an angular velocity of -w.

The tube containing blood and the blood fraction enters the fourth shaft from the top, and is looped into a U-shape so that it enters the center shaft from the bottom. Once the tube comes out from the top of the center shaft, it is connected to the chambers mounted on the centrifuge head.

Experimental Determination of the Natural Frequencies:

It turns out, purely by chance, that the two lowest natural frequencies of the existing device are very easily determined, because they occur in the process of bringing this device to the operating speed of 1500 rpm. There are two speeds at which the device undergoes large amplitude vibration, indicating resonance. With the aid of a stroboscope these speeds have been determined as 300 and 670 rpm. This provides an opportunity to check the validity of a simple lumped-parameter analytical model which will now be developed for predicting the corresponding natural frequencies.

DYNAMIC ANALYSIS:

It is a known fact that whenever any device passes through its natural frequency it experiences vibrations. Such vibrations could be desirable or undesirable. Dynamic analysis performed on any device helps us to predict analytically the natural frequencies. Depending on the values of the natural

frequencies so obtained, the operating regime for the device could be defined.

Figure 12 shows the simple three degree of freedom lumped-parameter torsional mode model of the cell separator. As seen from the figure, the model consists of six springs with stiffnesses represented by K's, moments of inertia of three lumped masses represented by I's, and the 0's represents the angular displacements. In the figure K" represent stiffnesses of belts, and K' represent stiffnesses of shafts.

For the model shown the equation of motion are,

i) $I_3\theta_3'' = -K_3\ (\theta_3 - \theta_2)$,

ii) $I_2\theta_2'' = -K_2\ (\theta_2 - \theta_1) + K_3\ (\theta_3 - \theta_2)$, and

iii) $I_1\theta_1'' = -K_1\theta_1 + K_1\ (\theta_2 - \theta_1)$.

To solve these equations, following procedure is used:

Let $\theta_1 = A_1\cos(wt)$,

$\theta_2 = A_2\cos(wt)$, and

$\theta_3 = A_3\cos(wt)$.

Therefore,

$\theta_1'' = -A_1w^2\cos(wt)$, (A)

$\theta_2'' = -A_2w^2\cos(wt)$, and (B)

$\theta_3'' = -A_3w^2\cos(wt)$. (C)

Substituting A, B, and C in the equations of motion and eliminating cos(wt) from these equations, we get a set of equations:

iv) $I_3w^2A_3 = K_3A_3 - K_3A_2$,

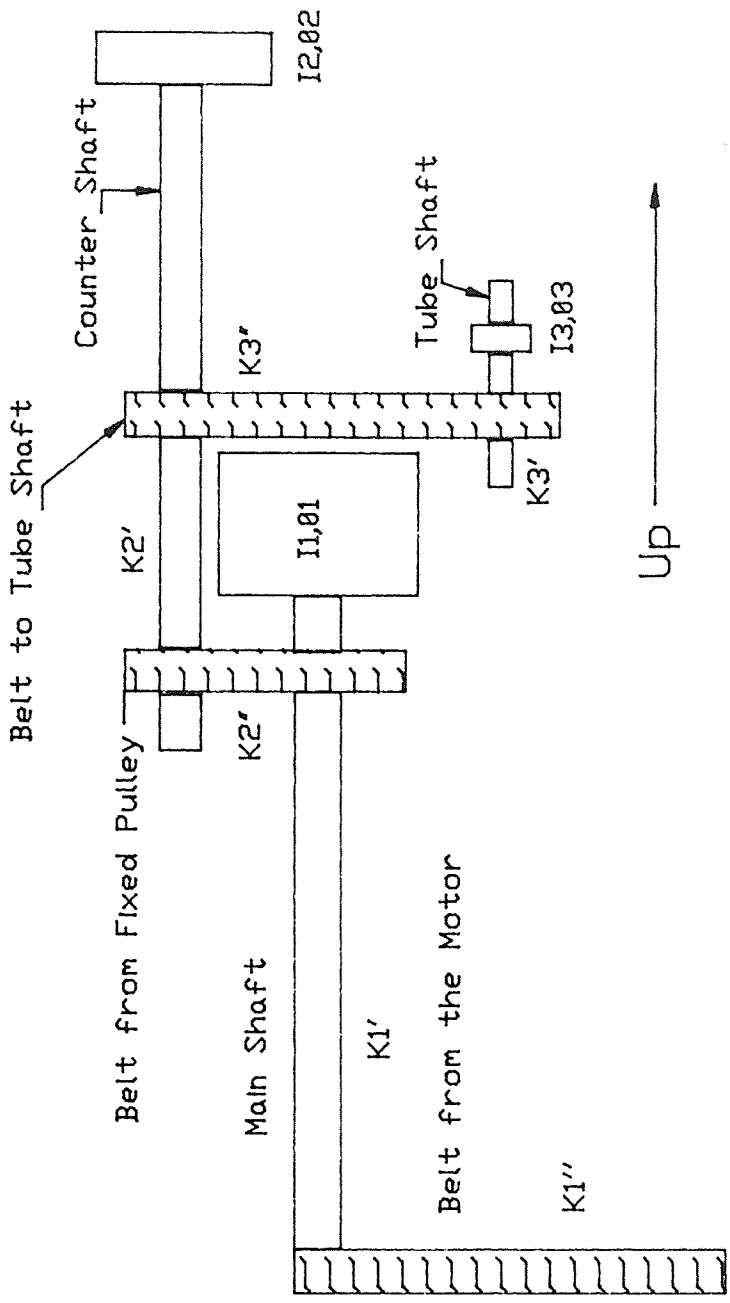

Fig. 12 Torsional mode model of the cell separator

v) $I_2w^2A_2 = (K_2 + K_3)A_2 - K_2A_1 - K_3A_3$, and

vi) $I_1w^2A_1 = (K_1 + K_2)A_1 - K_2A_2$.

Writing in the matrix notation we get,

$$\begin{bmatrix} I_1 & 0 & 0 \\ 0 & I_2 & 0 \\ 0 & 0 & I_3 \end{bmatrix} \begin{bmatrix} A_1 \\ A_2 \\ A_3 \end{bmatrix} \quad w^2 \quad = \quad \begin{bmatrix} (K_1 + K_2) & -K_2 & 0 \\ -K_2 & (K_2 + K_3) & -K_3 \\ 0 & -K_3 & K_3 \end{bmatrix} \begin{bmatrix} A_1 \\ A_2 \\ A_3 \end{bmatrix}$$

This is a system of equation of the form,

$$A\ X = \lambda M\ X.$$

All the constants involved in this set of equations are computed in Appendix(II).

Results and Discussion:

The above set of equations was solved using a computer program which used Jacobi method for evaluation of eigenvalues and eigenvectors. Output from the program is shown in Appendix(III).

As seen from the results, the lowest eigenvalue computed is about 37.29 rad/sec. This value also represents the fundamental frequency of the device. In terms of rotation per minute this is approximately 356 rpm. This value is comparable with the experimental value of 300 rpm. The value for second harmonic as computed from this model is about 88.19 rad/sec (i.e about 842 rpm).

This value is quite high as compared to the experimental value of second harmonic, which is about 660 rpm. A possible explanation for this occurrence could be that the second harmonic is arising from the combined effect of longitudinal

as well as torsional vibration. The second harmonic needs to be further analyzed. The third harmonic as shown by this model is very high. In fact it is well beyond the operating limit of this particular device, which is 1500 rpm.

The model, though, points out at some important facts. To avoid vibrations at low rpms the components going into the device must have low moments of inertia and high stiffnesses. Low moment of inertia means the components which are treated as masses must be light in weight, and the components which are treated as springs (like shafts, belts etc) must have high stiffnesses. In the proposed device, as far as possible all components are made from plastics instead of metals, and wherever possible stiffness of the component is increased by making it hollow. Further gear transmission would make this particular spring much stiffer than the belt.

The other thing that the calculations in Appendix(I) show is, the weight of the rotating parts in the proposed device is merely 3.50 lbs, as opposed to the existing device which has rotating mass of 6.25 lbs. This reduction in the rotating mass definitely indicates that the fundamental frequency of the proposed device in torsion will be very high than the existing one.

APPENDIX I

1) Carrier: Material for the carrier is Nylon 66 impregnated with carbon fiber. The density of this material is 0.046 $lb/inch^3$. Taking the dimensions from Fig.3,

weight of the top plate

$= \{10x5x0.25 - (3.142/4)[(0.75)^2 + (0.50)^2]x0.25\}x0.046$

$= 0.567$ lbs.

Similar procedure was carried out for the side and the bottom plate. The weights of these two components was found out to be 0.567 lbs and 0.106 lbs respectively. Hence the total weight of this component is 1.234 lbs.

Since there is a side plate with considerable thickness on one side of the assembly, the center of gravity of the carrier will not match with the assembly axis. This is going to cause a static imbalance.

c.g. of the carrier = (0.106 x 4.125) / (1.234)

= - 0.354 inches (negative since shift to the left)

Imbalance about the assembly axis = 1.234 x 0.354

= - 0.437 lb-inch.

M.I. of the carrier about its own c.g. (I_o),

$= [M ((l)^2 + (b)^2)] / 12$ (A)

where,

M = mass of the carrier,

l = length of the carrier, and

b = breadth of the carrier.

Hence,

$$\text{M.I.} = [\ (1.234/384)\ ((10)^2 + (5)^2)\ ]\ /\ 12$$

$$= 0.033 \text{ lb-inch-sec}^2$$

M.I. about the assembly axis is given by,

$$= I_o + M\ (d)^2 \qquad \text{(B)}$$

where d is the distance between the c.g. of the carrier and the assembly axis.

Hence, $\text{M.I.} = 0.033 + (1.235\ (0.354)^2\ /384)$

$$= 4.895\text{E-}04 \text{ lb-inch-sec}^2$$

2) Main Shaft : Material is nylon 66 impregnated with carbon fibers. Density of the material is 0.046 lb/(inch)^3. Taking dimensions from figure 4, the weight of this shaft is 0.093 lbs. Since the c.g of this shaft matches with the assembly axis there is no imbalance.

Moment of inertia of this shaft is

$$= (M/8)[(d_o^2 + d_i^2] \qquad \text{(C)}$$

where,

d_o = outer diameter of shaft, and

d_i = inner diameter of shaft.

So M.I. of the shaft is

$$= (0.093\ /(8\text{x}384))\ [\ (0.75)^2 + 0.375^2\ ]$$

$$= 2.128\text{E-}05 \text{ lb-inch-sec}^2$$

3) Idler gear and shaft assembly:

a) Idler gear: Material is Delrin. Density of the material is 0.0504 lb/inch^3. The dimensional details of the gear are, outer

diameter 0.75 inches, bore size 0.25 inches, and thickness of the gear 0.25 inches.

Using standard procedure of determining weight, the gear weighs 0.0049 lbs. M.I. of the gear about its own c.g. is given by equation (C) used above. Applying this equation M.I. of the gear is 9.96E-07 lb-inch-sec^2.

b) Idler shaft : The dimensions of idler shaft are, outer dia. 0.25 inches, inner dia. 0.156 inches, and the length of this shaft is 1.00 inches. Material for the shaft is teflon, which has the density of 0.0774 lb/inch^3.

Using above dimensions, weight of the shaft is found to be 0.023 lbs. M.I. of the shaft about its c.g. is computed using equation (C), and is found to be 6.50E-08 lb-inch/sec^2.

Total weight of idler gear and shaft assembly is,

= 0.0049 + 0.0023,

= 0.0072 lbs.

The M.I. of the entire assembly about its own c.g., is

= 9.96E-07 + 6.50E-08

= 1.061E-06 lb-inch-sec^2

This assembly is located at a distance of 1.875 inches from the assembly axis. Hence applying equation (B), M.I. of the entire assembly about assembly axis is found to be 6.69E-05 lb-inch-sec^2.

The net imbalance generated here is,

= (1.875 x 0.0072) = 0.0135 lb-inches

positive, since clockwise imbalance about assembly axis.

4) Compound gears and shafts:

a) Bottom Gear: Material for this gear is Delrin, the density of which is 0.0504 lbs/inch^3. The dimensional details are, pitch circle diameter 1.500 inches, bore size 0.50 inches, and thickness of 0.250 inches.

Using the dimensions mentioned above, and the density the weight of the gear is determined to be 0.0197 lbs. M.I. of this gear about its own c.g is determined by using equation (C) to be 1.612E-05 lb-inch-sec^2.

b) Top Gear: Material is Delrin, pitch circle diameter is 2.00 inches, bore size 0.50 inches, and thickness is 0.250 inches.

Weight of the gear computed is 0.039 lbs, and M.I about its own axis is 5.501E-05 lb-inch-sec^2.

c) Shaft: Material is Teflon. Other dimensional details of this shaft are, inner diameter 0.250 inches, outer diameter 0.50 inches, length of the shaft is 3.00 inches.

From these dimensions the weight of the shaft is computed as 0.0341 lbs. M.I. of the shaft about its own c.g. is found to be 3.92E-06.

The total weight of the entire assembly is 0.0927 lbs. The imbalance that it generates at a distance of 3.00 inches is 0.2781 lb-inch. Net M.I. of the whole assembly is 7.505E-05.

5) Bearings: Material for bearing is stainless steel. Density of the material is 0.286 lbs/inch^3. The dimensions of the bearings are given in Figure 7.

Weight of the bearing as computed is 0.01296 lbs. There

are two such bearings. Hence net weight is, 0.0259 lbs. These bearings are at a distance of 3.00 inches. Hence net imbalance these will generate is 0.0777 lbs-inch. There are other two bearings of same weight only at a distance of 1.875 inches. The net imbalance that these will generate is 0.0485 lbs-inches. Hence net imbalance generated because of bearings is, 0.1262 lb-inches.

The convention we follow is, anti-clockwise moment is negative while clockwise moment is positive. Thus except for the carriage, all other imbalances are positive.

Hence the sum of the positive imbalances is 0.4178 lb-inches. About 5% of the imbalance will also be generated by weights of bushings, nuts, screws and bolts going into the assembly. Hence the net positive imbalance is, 0.438, say approx. 0.44 lbs-inch.

As computed above, the negative imbalance coming from the carrier is 0.437 which is again approx. 0.44 lb-inch. Hence the device is statically balanced.

6) Head, Shaft and Gear configuration:

The head is made up of acrylic, the density of which 0.043 $lbs/inch^3$. It is 10 inches in diameter, with a bore of 2 inches at the center. Thickness of the head is 0.50 inches.

Using standard procedure, weight of the head is calculated to be 1.63 lbs, and M.I. is 0.0549 $lb\text{-}inch\text{-}sec^2$.

Shaft dimensions are, length 1.75 inches, inner dia. 0.375 inches, and outer dia. 0.75 inches. Material of the shaft is

Teflon. Hence weight of the shaft is 0.0458 lbs, and M.I 1.0485E-05 lbs-inch-sec^2. The gear is made of Delrin. The dimensions of the gear are, pitch circle dia. 4.0 inches, bore 0.75 inches, and face width 0.25 inches. Applying standard formulas, the weight of the gear is found to be, 0.1637 lbs, and M.I. is 8.82E-04 lbs-inch-sec^2.

Thus the net weight of this assembly is 1.8395 lbs, and the M.I. of the whole assembly is 0.05579 lbs-inch-sec^2. There is no imbalance @ assembly axis, since the c.g matches with the assembly axis.

APPENDIX II

Calculation of Stiffnesses:

1) K_1: This is the combination of stiffness of belt (K_1") and stiffness of the main central steel shaft (K_1'). Since K_1" and K_1' are in series, their combined stiffness is given by,

$$K_1 = (K_1' \times K_1'') / (K_1' + K_1'')$$

The computation of K_1" is done as follows:

Let K_{b1} represent the linear stiffness of the belt.

Therefore,

$$K_{b1} = (E \times w) / l_1$$

where

E: cross section modulus per inch of width = 25000 lb/inch.

w: width of the belt = 0.25 inch.

l_1: length of the belt = 11 inch.

Hence, $K_{b1} = (25000 \times 0.25) / 11$

$= 568.18$ lb/inch.

To find torsional stiffness we multiply K_{b1} by the radius of the pulley, say r_1.

i.e.,

$$K_1'' = (K_{b1} \times r_1^2)$$

$$= (568.18 \times (0.75)^2)$$

$= 319.60$ say approx 320 lb-inch/rad.

The computation of K_1' is done as follows:

$$K_1' = (J_1 \times G_s) / l_2$$

where

J_1 = polar moment of inertia for the steel shaft,

G_s = modulus of rigidity for steel = 10.6E06 psi, and

l_2 = length of the steel shaft = 5.75 inches.

Computation of polar moment of inertia:

$$J_2 = (3.142 \times d_1^4) / 32$$

$$= (3.142 \times (0.50)^4) / 32$$

$$= 6.135E\text{-}03 \text{ inch}^4 / \text{rad.}$$

In the above calculation d_1 is the diameter of the shaft.

Hence,

$$K_1' = (6.135E\text{-}03 \times 10.6E06) / 5.75$$

$$= 11301 \text{ lb-inch/rad.}$$

Substituting values of K_1' and K_1'' in equation of K_1 we get,

$$K_1 = (11301 \times 320) / (11301 + 320)$$

$$= 311.188 \text{ approx } 312 \text{ lb-inch/rad.}$$

2) K_2: This is the combination of stiffness of the belt (K_2'') and stiffness of the solid aluminum shaft (K_2'). Since K_2'' and K_2' are in series, their combined stiffness is given by

$$K_2 = (K_2' \times K_2'') / (K_2' + K_2'')$$

The computation of K_2'' is done as follows:

Let K_{b2} represent the linear stiffness of the belt.

Therefore,

$$K_{b2} = (E \times w) / l_3 ,$$

where

E= cross section modulus per inch of width = 25000 lb/inch,

w= width of the belt = 0.25 inch, and

l_3= length of the belt = 2.5 inch.

Hence, $K_{b2} = (25000 \times 0.25) / 2.5$

$= 2500$ lb/inch.

To find the torsional stiffness we multiply K_{b2} by the radius of the pulley, say r_2.

i.e. $K_2'' = (K_{b2} \times r_2^2)$

$= (2500 \times (0.50)^2)$

$= 625$ lb-inch/rad.

The computation of K_2' is done as follows:

$$K_2' = (J_2 \times G_a) / l_4$$

where

J_2 = polar moment of inertia for the aluminum shaft,

G_a = modulus of rigidity for aluminum = 4.0E06 psi, and

l_4 = length of the aluminum shaft = 4.75 inches.

Computation of polar moment of inertia:

$J_2 = (3.142 \times d_2^4) / 32$

$= (3.142 \times (0.25)^4) / 32$

$= 3.834E-04$ inch^4 / rad.

In the above calculation d_2 is the diameter of the shaft.

Hence,

K_2'= (3.834E-04 X 4.0E06) / 4.75

= 323 lb-inch/rad.

Substituting values of K_2' and K_2'' in equation of K_2 we get,

$$K_2 = (625 \times 323) / (625 + 323)$$

$$= 212.94 \text{ approx } 213 \text{ lb-inch/rad.}$$

3) K_3: This is the combination of stiffness of belt (K_3'') and stiffness of the hollow brass shaft (K_3'). Since K_3'' and K_3' are in series, their combined stiffness is given by

$$K_3 = (K_3' \times K_3'') / (K_3' + K_3'').$$

The computation of K_3'' is done as follows:

Let K_{b3} represent the linear stiffness of the belt. Therefore,

$$K_{b3} = (E \times w) / l_5 ,$$

where

E: cross section modulus per inch of width = 25000 lb/inch.

w: width of the belt = 0.25 inch.

l_5: length of the belt = 7.0 inches.

Hence, $K_{b3} = (25000 \times 0.25) / 7.00$

$= 892.85$ approx 893 lb/inch.

To find torsional stiffness we multiply K_{b3} by the radius of the pulley, say r_3.

i.e. $K_3'' = (K_{b3} \times r_3^2)$

$= (893 \times (0.50)^2)$

$= 223.25$ lb-inch/rad.

The computation of K_3' is done as follows:

$$K_3' = (J_3 \times G_b) / l_6,$$

where

J_3 = polar moment of inertia for the brass shaft,

G_b = modulus of rigidity for brass = 5.6E06 psi

l_6 = length of the brass shaft = 3.375 inches.

Computation of polar moment of inertia:

$$J_3 = (3.142 \times d_3^4) / 32$$

$$= (3.142 \times [(0.565)^4-(0.375)^4]) / 32$$

$$= 8.064E\text{-}03 \text{ inch}^4 / \text{rad.}$$

In above calculation d_3 is the diameter of the shaft.

Hence,

$$K_3' = (8.064E\text{-}03 \times 5.60E06) / 3.375$$

$$= 13{,}379 \text{ lb-inch/rad.}$$

Substituting values of K_3' and K_3'' in equation of K_3 we get,

$$K_3 = (13{,}379 \times 223.25) / (13{,}379 + 223.25)$$

$$= 219.58 \text{ approx } 220 \text{ lb-inch/rad.}$$

Calculation of Moment of Inertia:

a) M.I. of the first mass:

i) Bottom Structure: Figure 13 shows the elevation of the bottom structure. As seen from the figure the bottom structure consists of a plate, two blocks, and two pulleys. Figures 13 and 14 show the shape and dimensions for each of these components.

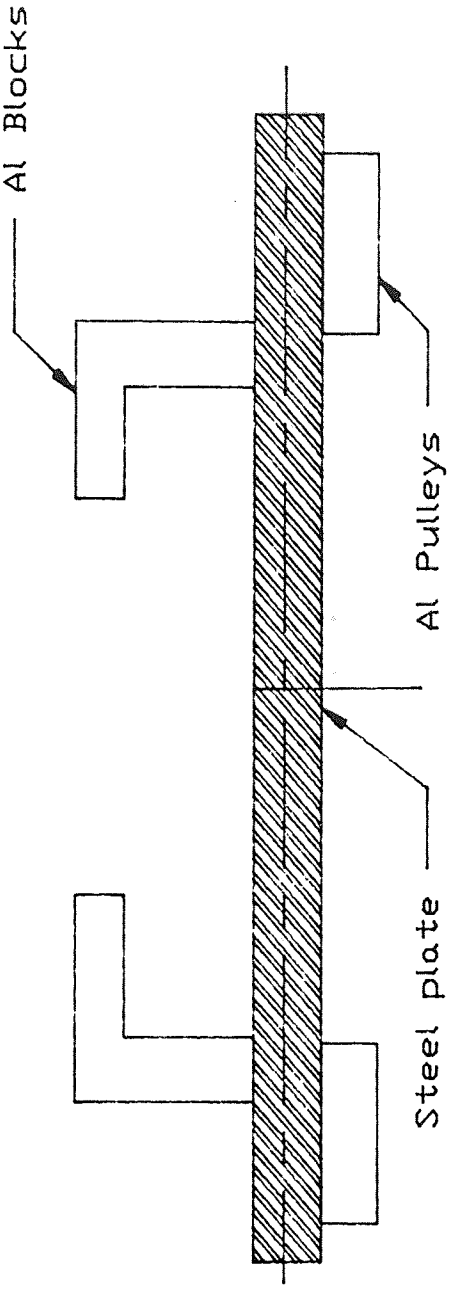

Fig. 13 Schematic of Bottom Structure

1) Moment of inertia of the plate:

Material of the plate : steel

density of the material = 0.286 lbs/inch^3

weight of the plate = volume of the plate X density

= [(6x2.25x0.25)x((6/2)x0.125x2x0.25] X 0.286

= 1.00 lb

weight of the hole = [(3.142x(0.50)^{2}x0.25x0.286]

= 0.0140 lb

net weight of the plate = 1 - 0.0140

= 0.9859 lb

center of gravity of the plate = 0.25/2 = 0.125 inches.

moment of inertia = [m(l^2 + b^2)/12]

= [0.9859((6)^2 + (0.25)^2)] / [384x12]

= 7.675E-03 lbs-inch^2

2) Moment of inertia of the aluminum block:

For the sake of convenience we divide the aluminum block in two rectangular blocks. The density of the Al is 0.100lb/inch^3

weight of first rectangle = 1.25x0.50x2.75x0.100

= 0.172 lb.

weight of the second rectangular block = 2.75x1.375x0.50x0.10

= 0.189 lb.

moment of inertia of the first block about its c.g.,

= (0.1718x[(0.50)^2 + (1.25)^2]) / (384x12)

= 6.722E-05 lb-inch-sec^2

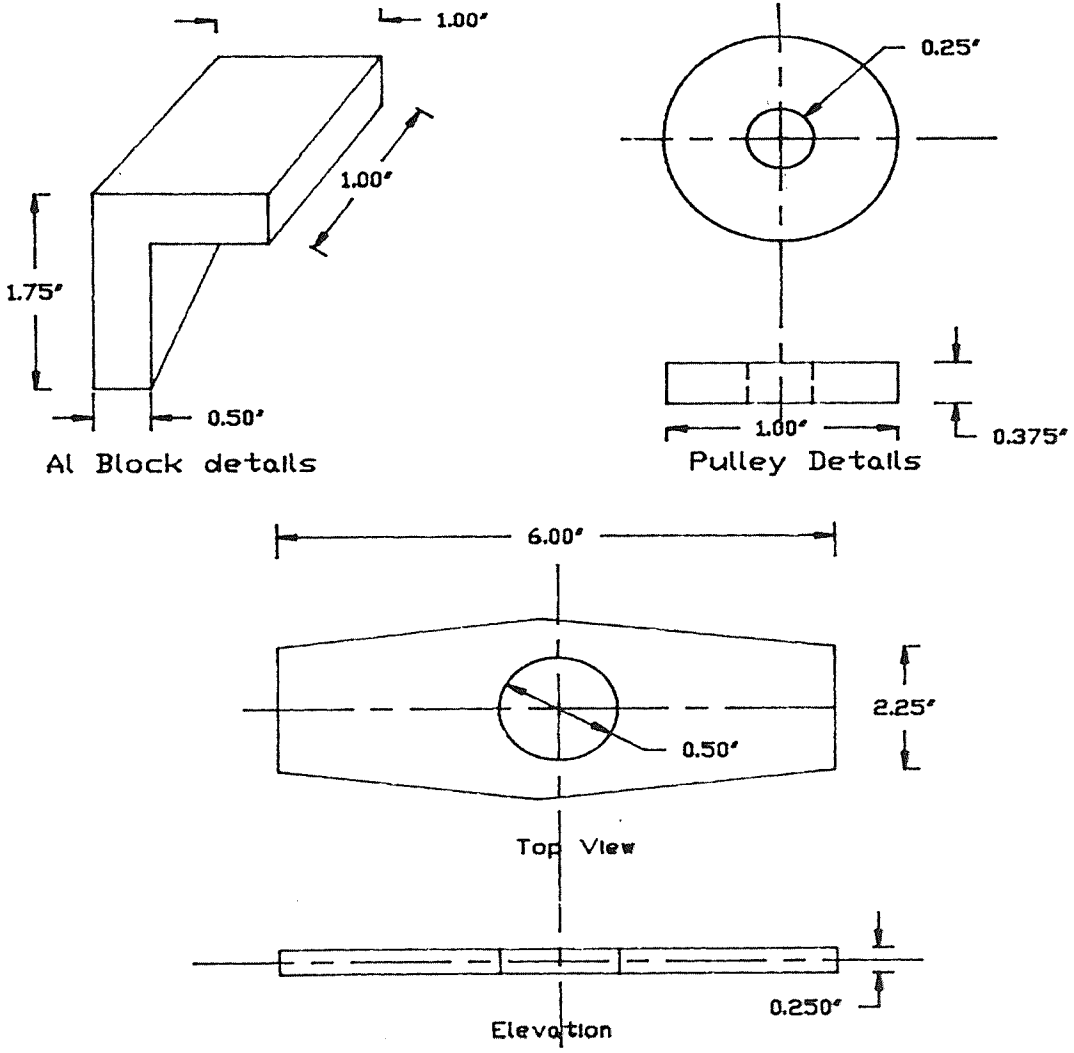

Fig. 14 Details of components on bottom structure

Moment of inertia about the assembly axis,

$$= I_o + (mxd^2)$$

where,

I_o is M.I. about its own c.g.,

m is the mass of the body, and

d is the distance from the assembly axis.

Hence, M.I. = $6.722E-05 + [(0.171/384)x(1.625)^2]$

$= 1.242E-03$ lb-inch-sec^2

Similar procedure was carried out for the second block, and moment of inertia was found to be = 7.778E-04 lb-inch-sec^2.

Hence the net MI of the two aluminum block is

$= 1.2442E-03 + 7.778E-04$

$= 2.022E-03$ lb-inch-sec^2

Such two aluminum blocks are there. Hence total M.I. of two blocks is 4.044E-03.

3) Pulleys: There are two pulleys. Material for pulleys is aluminum. Diameter of each pulley is 1 inch and width is 0.375inches.

weight of the pulley = $[3.142x(1)^2x0.375]x0.10 /4$

$= 0.0294$ lb.

weight of the hole = $[3.142x(0.25)^2x0.375]x0.10 /4$

$= 1.84E-03$ lb

Net weight of one pulley = 0.0294 - 1.84E-03

$= 0.02755$ lb

Moment of inertia of each pulley about its c.g.,

$$= (mxd^2)/8$$

$$= (0.0275x(1)^2) /(384x8)$$

$$= 8.95E\text{-}06 \text{ lb-inch-sec}^2$$

Moment of inertia about the assembly axis,

$$= I_o + (mx(dist)^2)$$

$$= 8.95E\text{-}06 + (0.02755x(2.25)^2)/384$$

$$= 3.72E\text{-}04 \text{ lb-inch-sec}^2.$$

Such two pulleys, and so total M.I.= 7.443E-04 lb-inch-sec^2.

Hence total M.I. of the bottom structure is,

$$= 7.675E\text{-}03 + 4.0446E\text{-}03 + 7.443E\text{-}04$$

$$= 0.0120 \text{ lb-inch-sec}^2.$$

ii) Top structure: The top structure consists of two plates, counter weight, gears and pulleys along with associated nuts and bolts. Figure 15 shows the schematic of entire assembly, while dimensional details and shapes of the associated components are shown in the figures 16 and 17.

1) Moment of inertia of the plates: Same procedure as shown above was used to determine the M.I. of the two plates. The dimensions of the plates are, length 12 inches, and thickness 0.25 inches. As seen from the figure there are three holes in the top and bottom plates. Material for the plate is steel.

Weight of each plate, approx 1.984 lb. Hence weight of two plates will be (1.984x2) 3.968, say approx 4 lbs. M.I. of the plate as computed from the similar procedure as the top structure is 0.1404 lb-inch-sec^2.

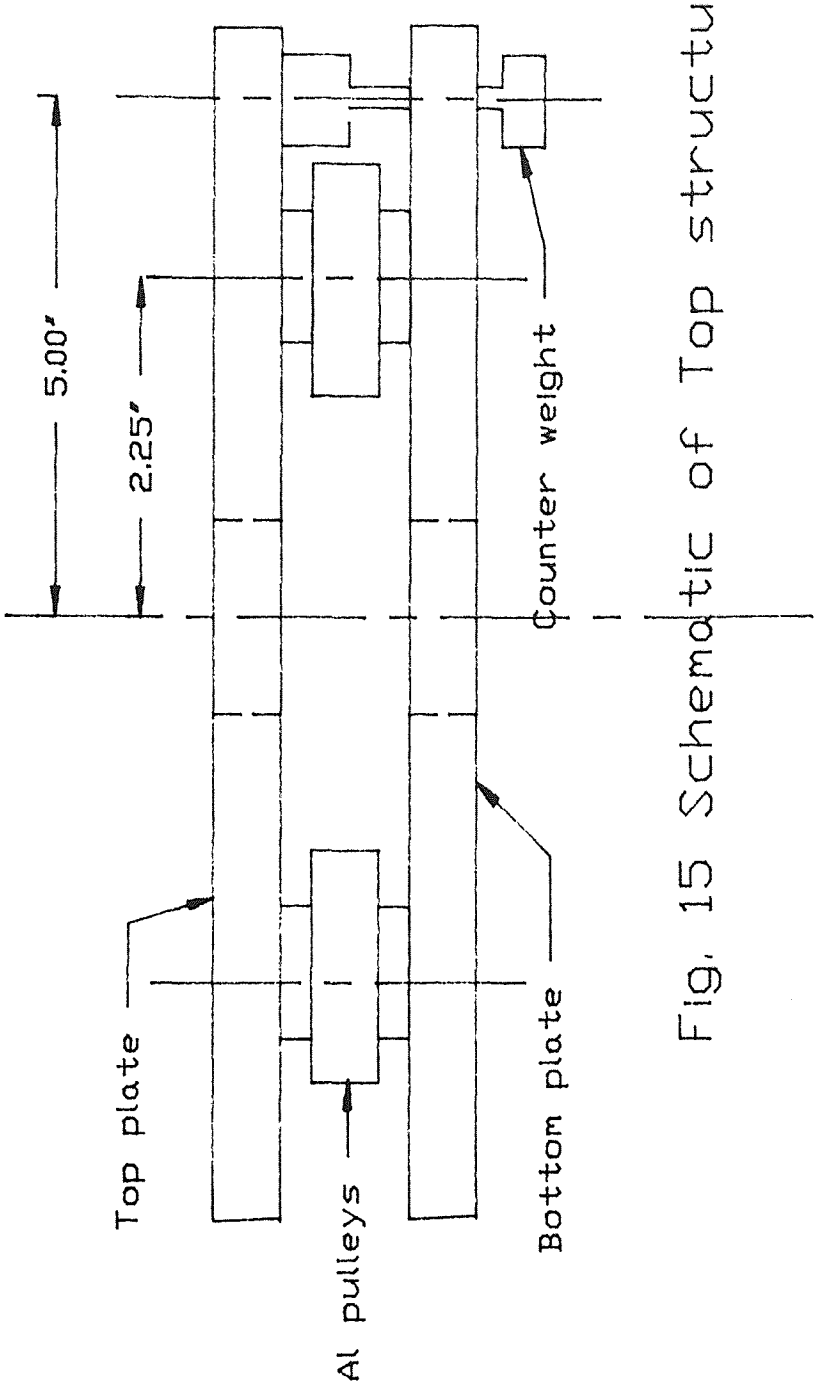

Fig. 15 Schematic of Top structure

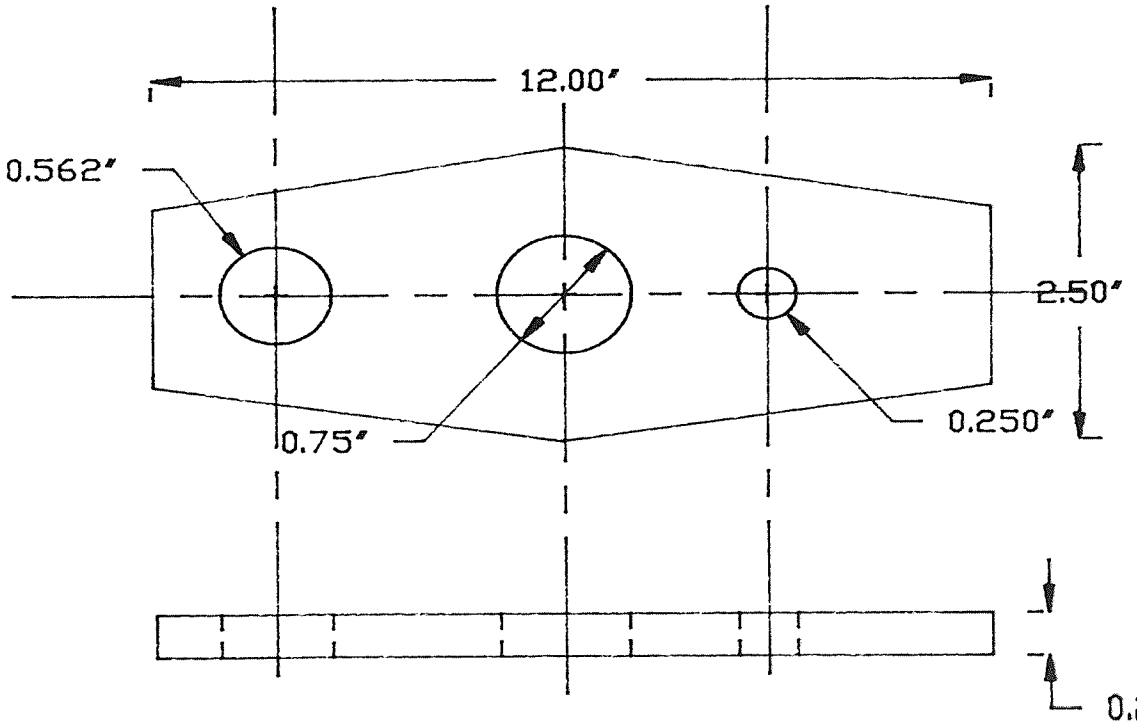

Fig. 16 Details of the Steel Plate

2) Moment of inertia of counter weights: Figure 17 shows dimensions and shape of the counter weight. Material for the counter weights is brass the density of which is 0.306 $lb/inch^3$. Following the standard procedure of determining weight, and moment of inertia we find M.I. of the counter weight to be 0.0253 $lb\text{-}inch\text{-}sec^2$.

3) Moment of Inertia of pulleys: Pulleys are of same dimension and material as that of the top structure. Hence M.I of the pulleys about its c.g is same as the pulleys on the bottom structure i.e 3.72E-04 $lb\text{-}inch\text{-}sec^2$, only they are located at different distance. One pulley is located at the distance of 5 inches, while other one is located at a distance of 2.50". Hence M.I. of first pulley is,

$$M.I. = 3.72E\text{-}04 + [(0.02755x(25))/384]$$

$$= 2.2656E\text{-}03\ lb\text{-}inch\text{-}sec^2$$

M.I. of the second pulley by the same procedure is, 8.204E-04.

Total moment of inertia of top structure is

$$= 0.1404 + 0.0253 + 2.2656E\text{-}03 + 8.204E\text{-}04$$

$$= 0.1687\ lb\text{-}inch\text{-}sec^2$$

Hence net M.I. of the first mass is

$$= 0.1687 + 0.0120$$

$$= 0.1807\ lb\text{-}inch\text{-}sec^2$$

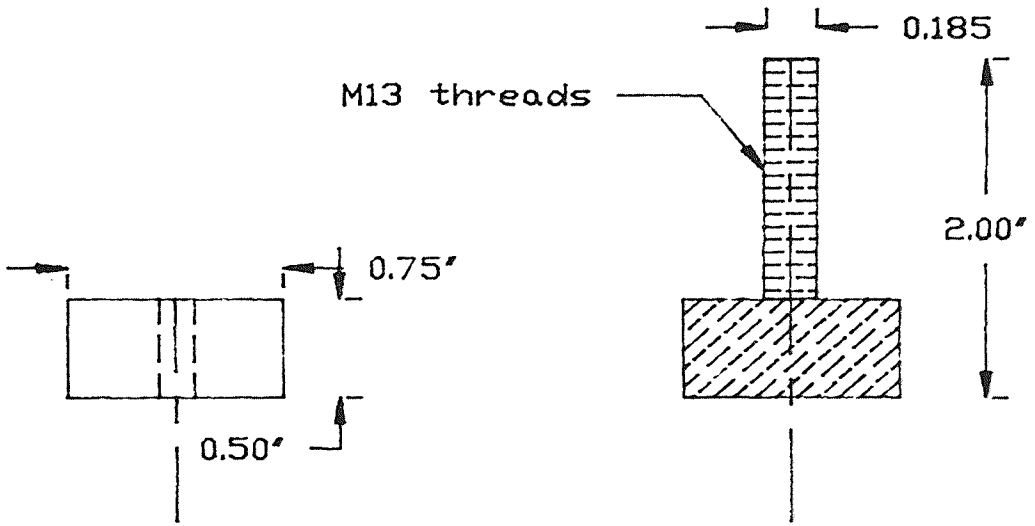

Fig. 17 Counter weight details

b) M.I. of the second mass:

Figure 18 shows the schematic of the assembly of head and chamber configuration.

1)Head and chamber configuration: Head is made up of acrylic material the density of which is 0.043 lb/inch^3. It is circular in shape with hole in the center. The diameter of the head is 8 inches, and thickness of the head is 0.75 inches. The diameter of the hole is 2 inches. Figure 19 shows the shape and dimension of the head and chamber. Applying standard formula M.I. is found to be 0.0334 lb-inch-sec^2.

2) Along with this there will also be M.I. of brass shaft which carries the head, collar and power transmitting gears.

Moment of inertia of the brass shaft, which weighs 0.3154 lbs is, M.I. = $(0.3154[(1)^2 + (0.75)^2]) / (8x384)$

= 1.604E-04 lb-inch-sec^2

Applying standard procedures, moment of inertia of the brass collar is found to be 2.91E-04 and two gears (which are made from Teflon) is found to be 1.662E-04.

Hence the M.I. of the second mass, which is summation of all the above M.I., is found to be 0.034 lb-inch-sec^2.

c) M.I. of the third mass:

This consists of hollow teflon shaft of length 4.5 inches. Shaft has inner diameter of 0.42 inches and outer diameter of 0.56 inches. Density of teflon is 0.079 lb/inch^3. Weight of this shaft is 0.0382 lbs.

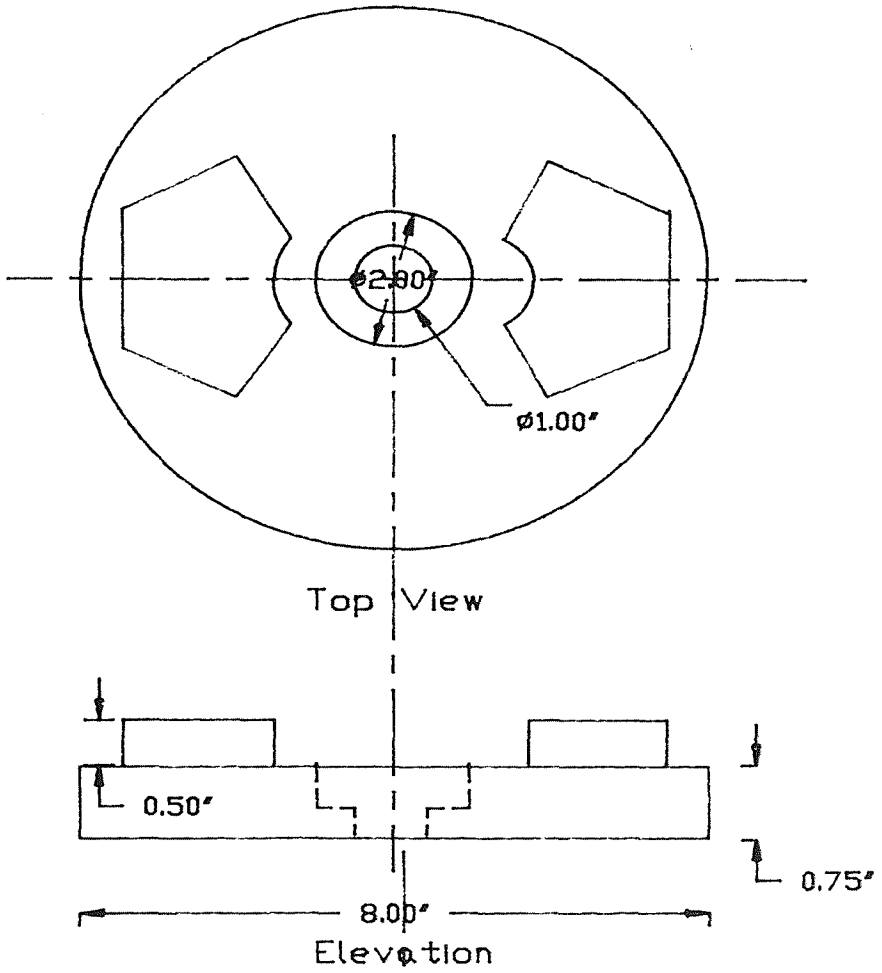

Fig. 18 Details of Head

M.I. of this shaft = $(0.0382 \times [(0.56)^2 + (0.42)^2]) / (384 \times 8)$

$= 6.075E\text{-}06$ lb-inch-sec^2.

APPENDIX-III

The stiffness matrix K is:

K(1, 1) = .5250000E+03

K(1, 2) = -.2130000E+03

K(1, 3) = .0000000E+00

K(2, 1) = -.2130000E+03

K(2, 2) = .4330000E+03

K(2, 3) = -.2200000E+03

K(3, 1) = .0000000E+00

K(3, 2) = -.2200000E+03

K(3, 3) = .2200000E+03

The mass matrix M is:

M(1, 1) = .1807000E+00

M(1, 2) = .0000000E+00

M(1, 3) = .0000000E+00

M(2, 1) = .0000000E+00

M(2, 2) = .3400000E-01

M(2, 3) = .0000000E+00

M(3, 1) = .0000000E+00

M(3, 2) = .0000000E+00

M(3, 3) = .6075000E-05

There were 0 rotations skipped on sweep number 1

```
There were  0 rotations skipped on sweep number  2
There were  0 rotations skipped on sweep number  3
There were  3 rotations skipped on sweep number  4
```

The scalar product of the first and last Eigenvectors of the transformed matrix is .00000000000000000

```
There were 4 sweeps performed.
The eigenvalues and eigenvectors follow:

Lambda ( 1) =            1390.3254
OMEGA( 1) =              37.2871 Rad/s          (A)

The associated eigenvector is:
  .1000000000D+01
  .1285296709D+01
  .1285346056D+01

Lambda ( 2) =            7778.6291
OMEGA( 2) =              88.1965 Rad/s          (B)

The associated eigenvector is:
  .1000000000D+01
```

```
 -.4134264221D+01
 -.4135152436D+01

Lambda ( 3) =        36220463.4772
OMEGA( 3) =            6018.3439 Rad/s          (C)

The associated eigenvector is:
  .5816272896D-08
 -.1787073809D-03
  .1000000000D+01
```

In above output, A, B, and C indicates the harmonics of the device. According to the presented model, the fundamental frequency, is at 37.29 rad/sec. In terms of rpm, this value is,

N = [(OMEGA) x 60] / [2 x pi]

= [37.29 x 60] / [2 x 3.142]

= 356.04 rpm approx 356 rpm.

Similarly from the second value of the OMEGA, we find that the second harmonic occurs at, 842.04 rpm or approx 842 rpm. Also third harmonic occurs at the third value of OMEGA, which in this case is well beyond the operating regime of the device.

BIBLIOGRAPHY

1) Van Wie, B.J., 1982, "Conceptualization and Evaluation of Techniques for Centrifugal separation of Blood cells: Optimum Process Condition, Recycle, and Stagewise Processing", A Dissertation submitted to the Graduate Faculty for the degree of Doctor of Philosophy at the University of Oklahoma, Norman.

2) Van Wie, B.J., 1979, "A continuous seal-less blood centrifuge for collection of blood components", A thesis presented for the Master of Science degree at the University of Oklahoma, Norman.

3) Van Wie, B.J., Sofer, S.S, 1985, "The effect of Recycle on the Continuous centrifugal processing of blood cells", International Journal of Artificial Organs, 8(1), 43-48.

4) Van Wie, B.J., Sofer, S.S, 1985, "Stagewise Separation to improve Continuous Centrifugal Blood Cell separator", International Journal of Artificial Organs, 8(1), 49-54.

5) Van Wie, B.J., Sofer, S.S, 1986, "Experimental consideration for the centrifugal separation of blood cell components", International Journal of Artificial Organs, 9(1), 49-58.

6) Roger Prescott, "Carbon Fibres", Modern Plastics Encyclopedia, 1988, pg. 183-184.

7) Folkes, M.J., 1982, Short Fiber Reinforced Thermoplastics, Research Studies Press., A division of John Wiley and Sons

Ltd., NY, USA.

8) Parker R.H, "Introduction to Injection Molding", Modern Plastics Encyclopedia, 1988 pg. 246-250.

9) Burton Paul,1979, Kinematics and Dynamics of Planar Machine, Prentice Hall Publishers, USA.

10) Cochin Ira, 1977, Analysis and Design of Dynamic Systems, Preliminary Edition, A Dun-Donnelley Publisher, NY, USA.

11) Cooney, D.O., 1976, Biomedical Engineering Principles-vol2, Marcell Decker Inc., New York, USA.

12) Dudley, 1984, Handbook of Practical Gear Design, McGraw Hill Book Company, NY, USA.

13) Ehrenstein, G.W., Erhard, G., 1984, Designing with Plastics, Hanser Publishers, Munich, West Germany.

14) Engineering Properties of Thermoplastics, A collective work produced by Imperial Chemical industries Ltd., edited by Ogorkiewicz, R.M., 1970, John Wiley and Sons, London, UK.

15) Lever, A.E., Rhys, J., 1958, The Properties and Testing of Plastic Materials, Chemical Publishing Company, NY, USA.

16) Mcfarlane, A.G.J, 1970, Dynamic System Models, George.G. Harrap and Company Ltd., England, UK.

17) Merriam, J.L, Kraige, L.G, 1987, Engineering Mechanics Volume(II): Dynamics, John Wiley and Sons Inc., USA.

18) Prentis, J.M, 1980, Dynamics of Mechanical Systems, Ellis Horwood Ltd., England, UK.

19) Seely Samuel, 1964, Dynamic System Analysis, Reingold Publishing Corp., NY, USA.

20) Shigley, J.E, 1967, Simulation of Mechanical Systems, McGraw Hill Book Company, NY, USA.

21) Stock Drive Products, 1987, Handbook of Small Standardized Components; Master Catalog 757.